

Article

Tackling Modeling and Kinematic Inconsistencies by Fixed Point Iteration-Based Adaptive Control

Awudu Atinga ^{1,*} and József K. Tar ^{1,2,3,†}

¹ Doctoral School of Applied Informatics and Applied Mathematics, Óbuda University, 1034 Budapest, Hungary; tar.jozsef@nik.uni-obuda.hu

² John von Neumann Faculty of Informatics, Óbuda University, 1034 Budapest, Hungary

³ Antal Bejczy Center of Intelligent Robotics, Óbuda University, 1034 Budapest, Hungary

* Correspondence: ugn9n8.uni-obuda.hu@stud.uni-obuda.hu

† Current address: Bécsi út 96/B, H-1034 Budapest, Hungary.

‡ These authors contributed equally to this work.

Abstract: The Fixed Point Iteration-based Adaptive Control design methodology is an alternative to the Lyapunov function-based technology. It contains higher-order feedback terms than the standard resolved acceleration rate control. This design approach strictly separates the kinematic and dynamic issues. At first, a purely kinematic prescription is formulated for driving the components of the tracking error to zero. Then an available approximate dynamic model is used to calculate the approximated necessary control forces. Before exerting on the controlled system, these forces are adaptively deformed in order to precisely obtain the prescribed kinematic behavior. The necessary deformation is iteratively found by the use of a contractive map that results in a sequence that converges to the unique fixed point of this map. In the case of underactuated systems, when the relative order of the control task also increases, the highest-order time-derivative depends on the lower-order ones according to the dynamic model of the system. This makes it impossible to realize the arbitrarily constructed kinematic design. In the paper, a resolution to this discrepancy is proposed. The method is demonstrated using two non-linear paradigms, a three-degree-of-freedom robot arm, and a two-degree-of-freedom system, i.e., two coupled non-linear springs. The operation of the method was investigated via simulations made by the use of Julia language and simple sequential programs. It was found that the suggested solution could be considered as a new variant of the fixed point iteration-based model reference adaptive control that is applicable for underactuated systems even if the relative order of the task is increased.

Keywords: adaptive control; fixed point iteration-based adaptive control; adaptivity by abstract rotations; Banach's fixed point theorem; model reference adaptive control



Citation: Atinga, A.; Tar, J.K. Tackling Modeling and Kinematic Inconsistencies by Fixed Point Iteration-Based Adaptive Control. *Machines* **2023**, *11*, 585. <https://doi.org/10.3390/machines11060585>

Academic Editors: Zheng Chen, Anthony Mandow, Raffaele Iervolino and Dariusz Horla

Received: 20 March 2023

Revised: 15 May 2023

Accepted: 16 May 2023

Published: 24 May 2023



Copyright: © 2023 by the authors. Licensee MDPI, Basel, Switzerland. This article is an open access article distributed under the terms and conditions of the Creative Commons Attribution (CC BY) license (<https://creativecommons.org/licenses/by/4.0/>).

1. Introduction

Using the humble capacities of the available electronic devices, in the 1980s, as a “model-based approach”, the idea of “Computed Torque Control (CTC)” was developed for robots [1,2]. To remove the mathematical complexities of the “Model Predictive Control (MPC)” that generally uses the dynamic model in the constraint terms of a complicated optimization task that worked well for slow chemical processes (e.g., [3–5]), in this approach the dynamic model is directly used for computing the necessary control torque or force components.

However, it became clear very early that, practically, it is impossible to develop precise enough dynamic models for robots (e.g., [6]). A reasonable control quality can be achieved by developing adaptive controllers that, based on real-time observations, compensate for the consequences of the imprecise models. A group of adaptive controllers tried to “learn the parameters of the exact models” (the appropriate prototypes are the “Slotine-Li Adaptive Robot Controller” and the “Adaptive Inverse Dynamics Controller (AIDC)” [7]). Instead of parameter tuning, the “Model Reference Adaptive Controller (MRAC)” approach introduced

fast feedback signals into the controlled system in order to make its dynamic behavior similar to that of a linear time-invariant “reference system” because it is easy to control such systems (early examples are, e.g., [8,9]). In the relatively fresh book chapter [10], it is stated that “Lyapunov’s direct method is introduced as an indispensable tool for analyzing the stability of nonlinear systems.” Really, the mainstream of designing adaptive controllers goes back to Lyapunov’s second method he elaborated in his Ph.D. dissertation in 1892 [11], which became well-known by the Western world only in the 1960s [12]. It is generally used in various adaptive solutions (e.g., [13,14]).

The Lyapunov function-based technique is prevalent, but it has some drawbacks.

1. The Lyapunov function-based design is not a simple algorithm that can be learned. It requires creative, mathematically well-educated designers. From the failure to find the appropriate Lyapunov function, no conclusions can be drawn regarding the solvability of the given problem, though for a large class of problems, appropriate *Lyapunov function candidates* are suggested for use (e.g., [15]).
2. It usually guarantees normal or asymptotic convergence of a scalar norm made of various error components that individually have physical interpretations and significance and should be driven to zero monotonically. However, the various components of this composite norm do not converge to zero monotonically, even if this norm itself monotonically vanishes.
3. Normally, complicated model terms must be precisely computed or at least estimated when this method is used.

In 2009, an alternative adaptive approach was initiated to tackle the above problems [16]. It can also be referred to as “Fixed Point Iteration-based Adaptive Control (FPIAC)”. Finding the appropriate control signal was transformed into iteratively computing the fixed point of the controlled system’s “Response Function”. This fixed point iteration-based approach individually keeps control of the selected error components by realizing some kinematically prescribed time-dependence for them.

In control technology, besides the lack of precise dynamic models, underactuation often causes practical problems. In a comprehensive survey of the underactuated mechanical systems [17], underactuation is defined as “An underactuated mechanical system (UMS) is a system which has fewer independent control actuators than degrees of freedom to be controlled.” (This concept, naturally, can be applied to a wider set of physical systems than Classical Mechanical ones). In addition to providing typical mechanical examples, this review classifies the underactuated systems according to the reasons for underactuation and system constraints (e.g., it considers holonomic and non-holonomic systems) by certain configuration characteristics and according to the related control problems. According to the state of the art at the time, the article mentioned the following methods which intended to control UMSs, including “Partial Feedback Linearization (PFL)” [18]; “Collocated PFL” [19]; “Non-collocated PFL” [20]; “Passivity-based Control (PBC)”, that is mainly used for setpoint regulation that is a narrow range of applications (e.g., for two-link manipulators [21], Furuta pendulum [22], and the so called TORA system [23]), its variants as “Interconnection and Damping Assignment Passivity-based Control (IDA-PBC)” [24], and the “Controlled Lagrangian” method [25]; “Backstepping Control” [26]; and “Sliding Mode Control” (e.g., [27], “Fuzzy Control” [28]). Due to its complexity, optimal control examples are not mentioned in our paper. A similar survey in 2018 concentrated on second-order underactuated systems [29], and extended the set of control methods with neural networks-based controllers [30].

The great majority of the above examples do not contain adaptive control. However, the adaptive ones as [28,31] are based on Lyapunov’s technique. To improve this situation, the possibility of using fixed point iteration-based adaptivity for underactuated systems was investigated in the earlier works and is further developed in this paper by revealing and tackling certain modeling inconsistencies that formerly were not considered. The main benefit of this approach is that by the use of quite primitive “approximate system models”, that may be realized by the use of simple embedded systems, quite complicated control tasks may be solved.

The paper is structured as follows: In Section 2, the closely related works are discussed. Section 3 contains the mathematically detailed problem formulation in two subsections depending on the existence of the need for developing a higher-order control approach in the control of the underactuated system. The simulation results and their noise sensitivity investigations are presented immediately after the description of the models. Section 4 summarizes the conclusions.

2. Related Work

In the previous works, the shortcomings of the Lyapunov function-based approach listed in Section 1 were addressed. For illustrating Shortcoming 1, i.e., mathematical complexity, **which is a simple structural issue**, the following paper provides a good example. In [32], a relatively simple system of the form of $\dot{x} = Ax(t) + bu(t) + bf(x(t), t)$ with state vector $x \in \mathbb{R}^n$, constant matrices with unknown elements $A \in \mathbb{R}^{n \times n}$, $b \in \mathbb{R}^{n \times 1}$, and an unknown bounded function $f(x, t)$ that represents the system non-linearities, model uncertainties, and the external disturbances was controlled. The authors provided a Lyapunov function-based solution using three special assumptions, five remarks, and two theorems, the mathematical details of which were expressed over pages 976–984 (approximately along 9 pages), and only the rest contained simulation results for a simple 2-degree-of-freedom system. Different Lyapunov functions were added in the complicated proof, which is a typical technique. The paper also serves as an example that normally, “observers” have to be developed for a Lyapunov function-based approach (Shortcoming 3).

In contrast to that, the fixed point iteration-based approach utilizes the fact that in a linear, normed, complete metric space (i.e., a Banach space) \mathcal{B} , the sequence generated by a *contractive* map $F : \mathcal{B} \mapsto \mathcal{B}$ so that $\{x_1; x_2 = F(x_1); \dots; x_{i+1} = F(x_i); \dots\}$ converges to the *unique fixed point of this function* $x_i \rightarrow x_* = F(x_*)$ as $i \rightarrow \infty$. The proof consists of a few simple lines.

By definition $F(x)$ is contractive if there exists $0 \leq K < 1$ so that $\forall x, y \in \mathcal{B} \|F(x) - F(y)\| \leq K\|x - y\|$. Since $\forall N \in \mathbb{N}$

$$\begin{aligned} \|x_{n+N} - x_n\| &= \|F(x_{n-1+N}) - F(x_{n-1})\| \leq K\|x_{n-1+N} - x_{n-1}\| \leq \dots \\ &\leq K^{n-1}\|x_{1+N} - x_1\| \rightarrow 0 \text{ as } n \rightarrow \infty . \end{aligned} \quad (1)$$

By definition $\{x_n\}$ is a Cauchy sequence that in a complete space converges to a limit value $x_* \in \mathcal{B}$. It is very easy to show that x_* is the fixed point of $F(x)$:

$$\begin{aligned} \|F(x_*) - x_*\| &= \|F(x_*) - x_n + x_n - x_*\| \leq \|F(x_*) - x_n\| + \|x_n - x_*\| \leq \\ &\leq K\|x_* - x_{n-1}\| + \|x_n - x_*\| \rightarrow 0 \text{ as } n \rightarrow \infty \text{ since } x_n \rightarrow x_* . \end{aligned} \quad (2)$$

Finally, the uniqueness of x_* can be easily proved by the indirect manner. Assume that two different fixed points of function $F(x)$ exist as $y_* \neq x_*$ so that $F(y_*) = y_*$ and $F(x_*) = x_*$. From this it follows that

$$\|y_* - x_*\| = \|F(y_*) - F(x_*)\| \leq K\|y_* - x_*\| \quad (3)$$

That is a contradiction if $\|y_* - x_*\| > 0$. The only contradiction-free solution is $y_* = x_*$.

In the control applications, the solutions occur in the vicinity of the fixed point; therefore, it is enough if the contractivity is valid in this restricted region.

Regarding Shortcoming 2, the following can be said. In control technology, often *quadratic Lyapunov functions* are constructed from the individual error components in the form $V(t) = \|e(t)\|^2 = e(t)^T P e(t)$ where P is a constant symmetric positive definite matrix. It evidently may happen that $V(t)$ can decrease while certain components of the error $e(t)$ increase in absolute value at the cost of the decrease in other components. Since the Lyapunov function-based technique concentrates on asymptotically driving $V(t)$ to zero, this property has significance in the “initial transient phase” of the control when $V(t)$ is big;

consequently, there may be large error components whose further growth is undesirable. Evading this problem in the fixed point iteration-based solution again is a simple **structural issue**. Instead of prescribing the behavior of some function $V(t) \in \mathbb{R}$, the time-dependence of certain components $e_i(t)$ is directly controlled. (There is no need for using and computing any Lyapunov function).

In general, a monotonic decrease in the individual error components can be prescribed kinematically in various manners. The typical PID-type feedback results in fluctuation with decreasing amplitude, while various fractional order calculus-based techniques realize a monotonic decrease with the given sign of the error components. These techniques are prevalent in robotics (e.g., [33,34]). In [35], an excellent review can be found on the history of fractional order calculus. In [36], fractional order calculus inspired sequences were combined with the fixed point iteration-based technique. Furthermore, in [37], a simple approach was suggested to simulate lower order control strategies for higher order systems to evade non-monotonic fluctuation of the error terms; a simple proportional error decay rate was simulated for a second order system. A control technology-based tackling of treating patients suffering from *type 1 diabetes mellitus*, an early version of this adaptive control, was investigated via simulations [38].

For evading the full state estimation that normally is necessary for the Lyapunov function-based design (Shortcoming 3), the FPI-based technique was applied to adaptively control a two-degree-of-freedom system in [39]. This system consisted of a wheel and a mass-point. The wheel's rotational position was the observed and controlled variable. The system contained some coupled "*parasite dynamics*"; along one of the spokes of the wheel, a mass point placed between two springs was able to move. However, its position (i.e., the directly not controlled variable) and velocity were not observable. The suggested method was able to control the wheel's rotational motion between certain physically determined limits without complete state estimation. The appropriate details of the present simulation are discussed as the properties of the dynamic models used in this paper.

As a heuristic method, MPC is still popular because it can be combined with different approximations. To evade the use of complicated non-linear solvers in vehicle lateral control in [40], the dynamic model of the system was removed from the cost function. Only the limitations of these kinematic terms were deduced from the dynamic model that, in fact, was used only in an inner loop. This structure is similar to the FPI-based approach that also separates the kinematic and dynamic terms. It can be expected that this method, later, can be combined with the FPI-based adaptive technique.

In the following sections, the problem formulation and the FPI-based design structure are detailed.

3. Problem Formulation and Development of the Design Structure

Mathematically, the method worked based on Banach's Fixed Point Theorem [41], which was briefly summarized in Section 2. The structure of this controller is described in Figure 1 for a system in which the " $\text{order} \in \mathbb{N}$ " time derivatives of the controlled coordinates the control force can instantaneously set. The method is designed for *digital controllers* in which the delay corresponds to the duration of the control cycle. In the "*Kinematic Block*", various ideas can be applied that produce a "*desired*" $q^{(\text{order})\text{des}}$ time-derivative that should be realized in order to drive the selected error components to zero.

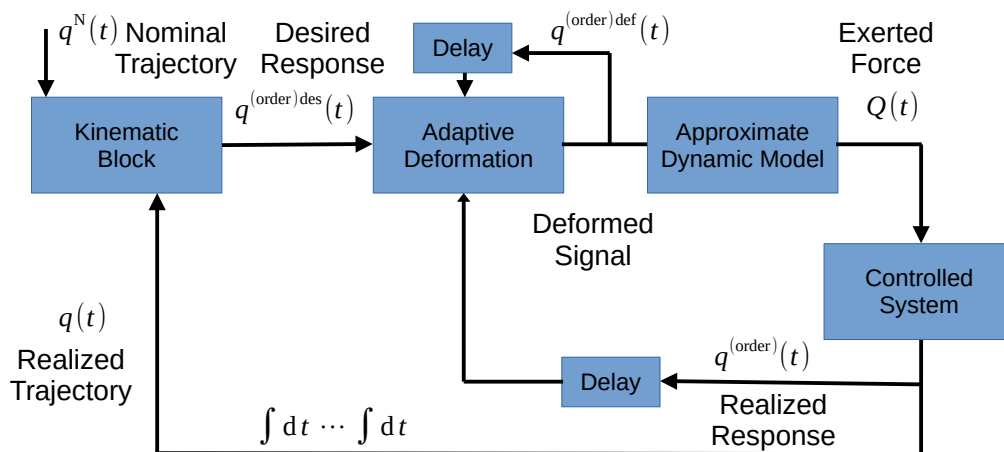
It is evident that if the block "*Adaptive Deformation*" is removed from Figure 1, we arrive at the original CTC control. In the lack of the possession of a precise model, some available approximate dynamic models were used for calculating the necessary control force $Q(t)$ that is exerted on the controlled system, the response of which is the *realized time-derivative* $q^{(\text{order})}(t)$. The function of the block called "*Adaptive Deformation*" is deforming the input

of the “Approximate Model” (denoted by $\tilde{\mathcal{M}}$) to achieve the case $q^{(order)des} = q^{(order)}$. This equation can be approximated as

$$Q = \tilde{\mathcal{M}}(q, \dot{q}, \dots, q^{(order-1)}, q^{(order)des}) \tag{4a}$$

$$q^{(order)} = \mathcal{M}^{-1}(q, \dot{q}, \dots, q^{(order-1)}, Q) \text{ leading to} \tag{4b}$$

$$q^{(order)} \cong \mathcal{M}^{-1}(\tilde{\mathcal{M}}(q^{(order)des})) = f(q^{(order)des}) , \tag{4c}$$



The FPI-based Adaptive Controller

Figure 1. The structure of the higher order Fixed Point Iteration-based Adaptive Controller for fully actuated system (after [16]).

It was taken into account that while the control force can immediately modify $q^{(order)}$, the other coordinate derivatives vary relatively slowly. In this manner, the *response function* $f(q^{(order)des})$ was introduced as an approximation. In practical applications, the *approximate dynamic model* $\tilde{\mathcal{M}}$ is known, but the *exact inverse model* \mathcal{M}^{-1} is unknown. We should like to achieve the value $f(q^{(order)des})$. Assume we are near x_* that yields $f(x_*) = x^{des}$, and let α be some real number. Try to use the iteration

$$x_{i+1} = x_i + \alpha(x^{des} - f(x_i)) ,$$

$$f(x_i) = f(x_* + x_i - x_*) \cong x^{des} + \frac{\partial f}{\partial x}(x_i - x_*) \text{ from which it follows that} \tag{5}$$

$$x_{i+1} - x_* \cong \left[I - \alpha \frac{\partial f}{\partial x} \Big|_{x_*} \right] (x_i - x_*) .$$

Evidently, if the matrix $\left[I - \alpha \frac{\partial f}{\partial x} \Big|_{x_*} \right]$ is *contractive*, the $x_i \rightarrow x_*$ convergence can be guaranteed. Consider the variation of the norm of a transformed array w as

$$\|[I - \alpha M]w\|^2 = \|w\|^2 - \alpha w^T (M + M^T)w + \alpha^2 w^T M^T M w \tag{6}$$

in which for small α the quadratic term can be neglected, so the second term must give a negative contribution. With the analogy of the monotonic function, the function $f : \mathbb{R}^n \mapsto \mathbb{R}^n$ can be regarded as *approximately differentially direction keeping* if for all Δx

$$\Delta x^T \Delta f = \Delta x^T (f(x + \Delta x) - f(x)) \cong \Delta x^T \frac{\partial f}{\partial x} \Delta x > 0, \tag{7}$$

that is, the angle between the vectors Δx and Δf is acute. Since any matrix, in our case $\frac{\partial f}{\partial x}$, can be decomposed into a symmetric and a skew symmetric part, and the latter does not give a contribution to $\Delta x^T \Delta f$ in Equation (7), it can be understood that in many applications convergence can be achieved if such a sequence is realized, e.g., in the box “Adaptive Deformation” with the inputs as follows, **the actual desired value** $x^{des} \equiv q^{(order)des}$; **the deformed value in the previous control cycle** $q^{(order)def}$; and **the response obtained for the previously applied control input** $q^{(order)}$ that are available in the given time instant due to the delay. Because, in general, it is difficult to determine the appropriate value of parameter α , various constructions were suggested for the deformation in [16,42,43]. They have various parameters by the setting of which the convergence of the iteration can be guaranteed if the system model allows it mathematically.

The most straightforward solution was announced in [44], which tries to move the response $f(x_i)$ toward x_{i+1}^{des} in the following manner. At first, it augments the dimension of these vectors with additional physically not interpreted components so that the augmented vectors have the same Frobenius norm. It then constructs a rotation operator in the augmented space that rotates the augmented $f(x_i)$ into the augmented x_{i+1}^{des} by leaving the vectors in their orthogonal subspace (this corresponds to a higher dimensional rotational axis) invariant. The similarly augmented version of x_i is created and rotated with a fragment of the original rotation angle around the same rotational axis. Consequently, the physically interpreted projection of the rotated vector moves toward the desired direction, and, in this case, the interpolation factor λ_n can be placed in the interval $[0, 1]$. Figure 2 intuitively describes the method. In [45], the original version published in [16] was combined with a genetic algorithm in order to optimize its parameters.

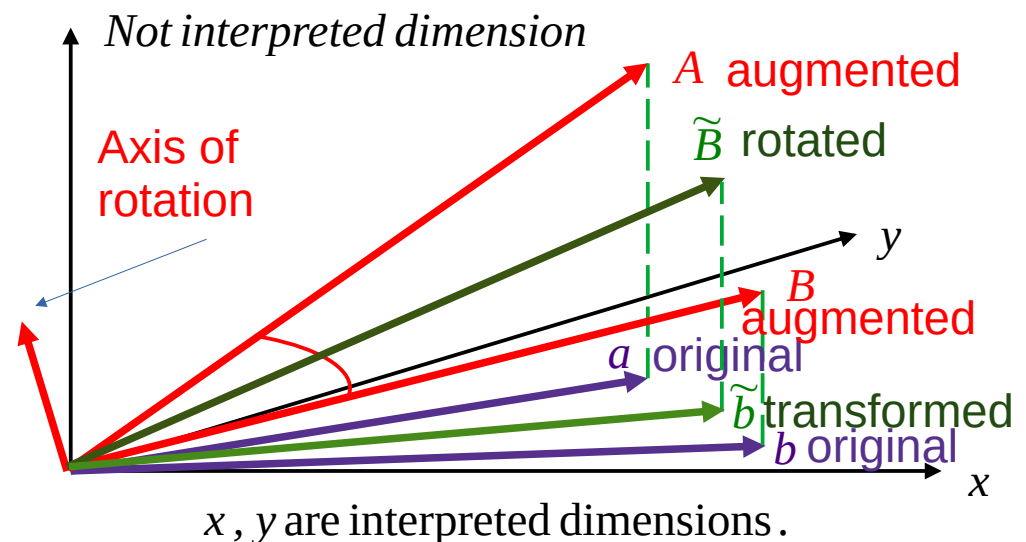
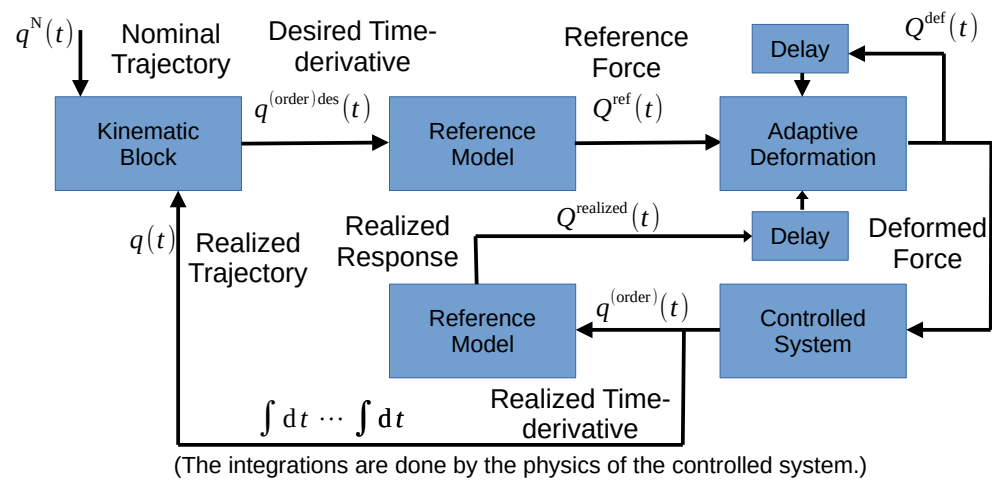


Figure 2. Symbolic description of the abstract rotations in the adaptive deformation (after [44]).

In [46], it was realized that if the adaptive iterative deformation is moved from the space of the derivatives to that of the generalized forces, a novel, “Fixed Point Iteration-based Adaptive MRAC controller (FPI-based MRAC)” can be developed for fully actuated systems as it is indicated in Figure 3. The purely kinematic design in the “Kinematic Block” continues the calculation with the dynamic data of the reference model. If the iteration converges in the space of the generalized forces, it has the illusion that the controlled system’s dynamics is identical to that of the reference model. This latter can be a generally non-linear model, in contrast to the linear time-invariant reference model of the Lyapunov function-based design. For convergence, the same argumentation can be applied as in the case of the previous controller. The already systematically investigated applications of the above methods were made for fully actuated systems; however, in practice often can be found underactuated systems, the control of which is an exciting issue. The investigations

summarized in the sequel are the first systematic studies that reveal not only *modeling imprecisions* but also **modeling and kinematic inconsistencies** concerning the application of the fixed point iteration-based adaptive control for underactuated systems. These problems are revealed and tackled in the sequel.



The FPI-based Model Reference Adaptive Controller for Full Actuation

Figure 3. The scheme of the Fixed Point Iteration-based MRAC controller for fully actuated systems (after [46]).

3.1. Suggested Controller Structures for Underactuated Systems without and with Increased Relative Order

Underactuation generally means that the number of independent control signals is smaller than that of the degree of freedom of the controlled system. Consequently, in this case, it is impossible to control the motion of each axle; specific axles will move *as they want*. However, the motion of a given directly not actuated axis can be controlled by the control force/torque exerted on a given directly actuated axis. It depends on the nature of the particular task if this solution will increase or not increase the *control task's relative order*. In this paper, both cases are investigated using two simple paradigms. The first is a robot arm in which the driver of one of the axles is corrupted and allows the appropriate axis to rotate freely. In this case, the relative order of the control is not increased. The other example consists of two linearly moving, dynamically coupled springs with mass points so that on the second (lower) mass point, no direct control force can be exerted. Its motion can be influenced by the force term directly acting on the first (upper) mass point, the motion of which is coupled to that of the lower mass point via viscous friction. In this case, the relative order of the control is increased from 2 to 3. This simple model represents a class of similar problems, e.g., in the “Pneumatic Artificial Muscle (PAM)” actuator, similar components are present that may cause oscillations (e.g., [47,48]). In [48], a method similar to the CTC control was applied for position control. If several pieces of the lower spring and mass systems are connected to the upper one so that, as parasite dynamics, they perturb its motion, the model of a multi-cantilever-mass mechanism can be developed. In [49], only linear springs were considered, and the main point was vibration suppression.

3.2. Control of a Corrupted 3D Puma-Type Robot Arm (Problem without Increasing the Relative Order of the Controller)

The dynamic model of the first three axles of a PUMA-type robot was investigated in [50], in this paper a relatively simple, corrupted version of this model will be used. Its kinematic structure is described in Figure 4.

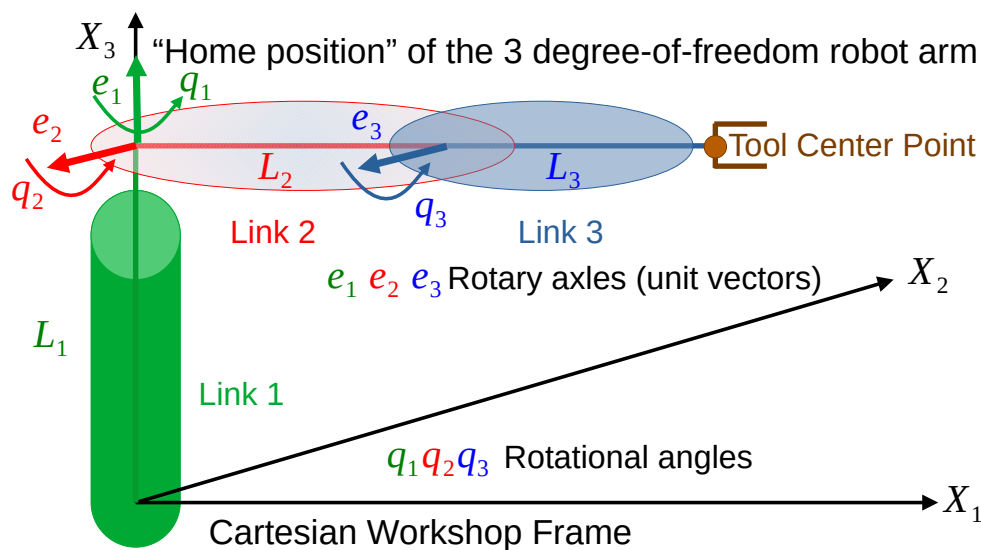


Figure 4. The kinematic structure of the 3D robot arm in the “home position” (after [50]).

It is assumed that the motion of the axes q_1 and q_2 can be directly controlled by the torque values Q_1 and Q_2 , but the drive of the link of length L_3 is corrupted, therefore $Q_3 \equiv 0$. The following control compromise is applied, a *nominal trajectory to be tracked* is defined as $\dot{q}_1^N \equiv \text{const.}$, and $q_3^N(t) \equiv \text{const.}$ motion. The suggested control structure seems to be the modification of the FPI-based MRAC controller in which the available approximate model takes the role of the reference model (Figure 5). By the use of the $Q_3 \equiv 0$ equation for the approximate model \ddot{q}_2^{des} can be computed and after that can be utilized for the calculation of Q_1^{appr} and Q_2^{appr} . The dynamic and kinematic parameters of the robot arm are given in Table 1, the equations of motion (after [50]) are given in Equation (8).

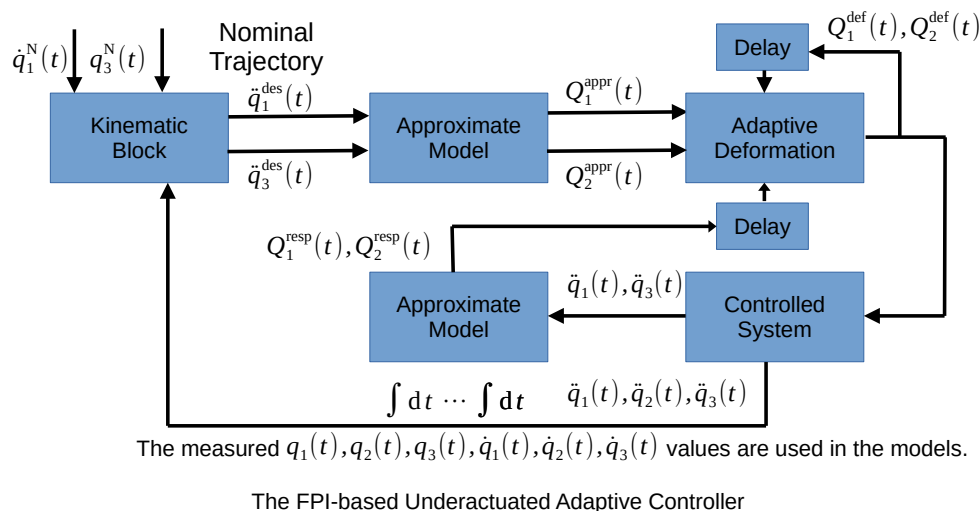


Figure 5. The control structure for the corrupted 3D robot arm.

Table 1. The kinematic and dynamic parameters of the robot arm (after [50]).

Parameter	Measurement Unit	Exact Value	Approx. Value
Length of Link 2: L_2	[m]	1.0	1.0
Length of link 3: L_3	[m]	2.0	2.0
Mass of link 2: m_2	[kg]	10.0	15.0
Mass of link 3:	[kg]	20.0	25.0
Gravitational acceleration g	$[m \cdot s^{-2}]$	9.81	9.81
Moment of inertia of link 1: Θ	$[kg \cdot m^2]$	50.0	60.0

$$H(q)\ddot{q} + h(q, \dot{q}) = Q, \text{ leading to} \tag{8a}$$

$$Q_1 = \left[\Theta_1 + \frac{1}{4}m_2L_2^2c_2^2 + \frac{1}{4}m_3L_3^2c_{23}^2 + m_3L_2^2c_2^2 + \frac{1}{2}m_3L_2L_3c_{23}c_2 \right] \dot{q}_1 + \left[-\frac{1}{2}m_2L_2^2c_2s_2\dot{q}_2 - \frac{1}{2}m_3L_3^2c_{23}s_{23}(\dot{q}_2 + \dot{q}_3) - 2m_3L_2^2c_2s_2\dot{q}_2 - \frac{1}{2}m_3L_2L_3s_{23}c_2(\dot{q}_2 + \dot{q}_3) - \frac{1}{2}m_3L_2L_3c_{23}s_2\dot{q}_2 \right] \dot{q}_1, \tag{8b}$$

$$Q_2 = \left[\frac{1}{4}m_2L_2^2 + \frac{1}{4}m_3L_3^2 + m_3L_2^2 + \frac{1}{2}m_3L_3L_2c_3 \right] \dot{q}_2 - \frac{1}{2}m_3L_3L_2s_3\dot{q}_3\dot{q}_2 + \left[\frac{1}{4}m_3L_3^2 + \frac{1}{4}m_3L_3L_2c_3 \right] \dot{q}_3 - \frac{1}{4}m_3L_3L_2s_3\dot{q}_3^2 + \left[\frac{1}{4}m_2L_2^2c_2s_2 + \frac{1}{4}m_3L_3^2c_{23}s_{23} + m_3L_2^2c_2s_2 + \frac{1}{4}m_3L_2L_3s_{23}c_2 + \frac{1}{4}m_3L_2L_3c_{23}s_2 \right] \dot{q}_1^2 + \frac{1}{2}m_2L_2g c_2 + m_3g L_2c_2 + \frac{1}{2}m_3L_3g c_{23}, \tag{8c}$$

$$Q_3 = \left[\frac{1}{4}m_3L_3^2 + \frac{1}{4}m_3L_3L_2c_3 \right] \dot{q}_2 + \frac{1}{4}m_3L_3^2\dot{q}_3 + \left[\frac{1}{4}m_3L_3^2c_{23}s_{23} + \frac{1}{4}m_3L_3L_2s_{23}c_2 \right] \dot{q}_1^2 + \frac{1}{4}m_3L_3L_2s_3\dot{q}_2^2 + \frac{1}{2}m_3g L_3c_{23}. \tag{8d}$$

It has to be noted that not only the definition of the “home position of the robot” is different to that of [1], but the mass distribution of the components is different, too. Faitli used a simple “rod model” in which the masses were concentrated at half length of the rods. This model lead to $H_{12} = H_{21} = 0$, $H_{13} = H_{31} = 0$, and considerable H_{11} , H_{22} , and $H_{23} = H_{32}$ terms. Due to the more realistic mass distribution used, in [1] relatively little $H_{12} = H_{21}$ and $H_{13} = H_{31}$ terms occur, too. This difference does not concern the logic of the controller design.

For the kinematic block, if the tracking error is $e(t) := q^N(t) - q(t)$, and $e_{int}(t) := \int_{t_0}^t e(\xi) d\xi$, the following tracking properties can be described with the positive constants Λ_1 and Λ_3 :

$$\left(\Lambda_1 + \frac{d}{dt} \right) \dot{e}_1(t) \equiv 0 \text{ yielding } \ddot{q}_1^{des}(t) = \Lambda_1 \dot{e}_1(t) + \ddot{q}_1^N(t), \tag{9a}$$

$$\left(\Lambda_3 + \frac{d}{dt} \right)^3 e_{int3} \equiv 0 \text{ yielding } \ddot{q}_3^{des}(t) = \Lambda_3^3 e_{int3}(t) + 3\Lambda_3^2 \dot{e}(t) + 3\Lambda_3 \dot{e}(t) + \ddot{q}_3^N(t). \tag{9b}$$

The same iteration happens as in the case of the FPI-based MRAC controller. Physically it can be expected that via some fluctuation of $q_2(t)$, the axis $q_3(t)$ can be kept fluctuating around the constant nominal value prescribed for it. Due to the presence of gravity the existence of “static solution” cannot be expected.

To tackle the problem of measurement noises occurring in measuring the joint coordinates q_1, q_2, q_3 , in the calculation of the control force, a simple low pass filter was used (even in the case of the noise-free simulations, too) in the following manner. The *measured/observed noisy value of the exact coordinate $q(t)$* was $q^o(t) = q(t) + \mathcal{N}(t)$, in which the additional noise term corresponded to a random Gaussian noise of zero mean and $\sigma = 10^{-5}$ rad standard deviation. Instead of $q^o(t)$ and its numerical derivatives, the *smoothed value $q^s(t)$* was utilized that satisfied the differential equation

$$\left(\lambda_s + \frac{d}{dt}\right)^3 q_i^s(t) = \lambda_s^3 q_i^o(t) \quad (10)$$

with the initial conditions $q_i^s(t_0) = q_i(t_0) = 0$, $\dot{q}_i^s(t_0) = \dot{q}_i(t_0) = 0$, and $\ddot{q}_i^s(t_0) = \ddot{q}_i(t_0) = 0$ with $\lambda_s = 10^3$ [s⁻¹]. Such a filtering may cause some delay even in the lack of the measurement noises.

The computation of the Q_1^{appr} and Q_2^{appr} force components in the block “Approximate Model” of Figure 5 happens in the following manner. Consider Equation (8) and

1. Fill it in with the parameters of the *available approximate model* and the *actually measured (noise-filtered) values* of the variables q_1^s, q_2^s, q_3^s , and $\dot{q}_1^s, \dot{q}_2^s, \dot{q}_3^s$;
2. Substitute $Q_3 = 0$ and \ddot{q}_3^{des} into Equation (8d) and calculate \ddot{q}_2^{des} ;
3. Substitute \ddot{q}_2^{des} and \ddot{q}_3^{des} into Equation (8c) and calculate Q_2^{appr} ;
4. Substitute \ddot{q}_1^{des} into Equation (8b) and calculate Q_1^{appr} .

The lower “Approximate Model” block works in similar manner.

For the simulations the following data given in Table 2 were used:

Table 2. Controller and simulation data for the robot arm.

Parameter	Measurement Unit	Value
Digital time resolution: δt	[s]	10^{-3}
Noise filtering parameter λ_s	[s ⁻¹]	10^3
Adaptive interpolation parameter λ_a	[nondimensional]	0.9
Trajectory tracking parameter Λ_1	[s ⁻¹]	4.0 and 8.0
Trajectory tracking parameter Λ_3	[s ⁻¹]	4.0 and 8.0
Norm of augmented vectors R_a	[N · m]	10^4
σ of Gaussian noise	[rad]	0 and 10^{-5}

3.2.1. Simulations without Measurement Noise

The initial transient part during which the initially zero \dot{q}_1 and q_3 approach their nominal values as well as the fluctuations with which they are kept near the prescribed nominal value depends on the parameters Λ_1 and Λ_3 . These phases can be well identified in Figure 6. The common norm of the augmented vectors was $R_a = 10^4$ [N · m], and the interpolation factor of the adaptivity was $\lambda_a = 0.9$. The time resolution of the simulations (i.e., assumed cycle time of the digital controller) was $\delta t = 10^{-3}$ s, and the simplest Euler integration was applied.

Figure 7 reveals the control forces, the motion of the controlled axle q_2 , and the angle of the adaptive deformation φ . Evidently, considerable adaptive deformation was necessary to compensate for the effects of the modeling errors.

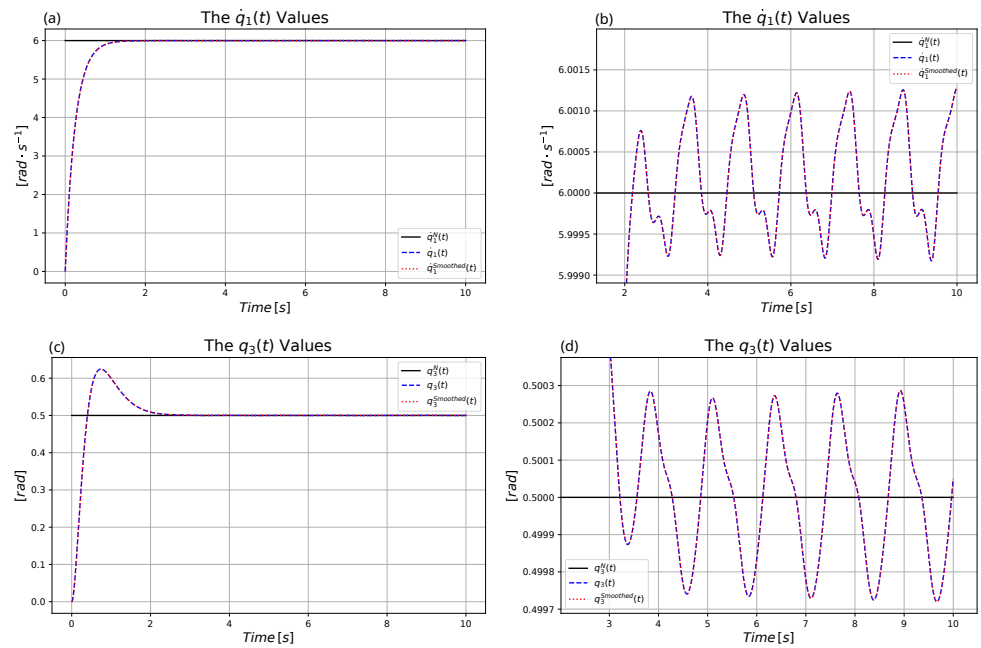


Figure 6. The nominal and realized motion for $\Lambda_1 = \Lambda_3 = 4.0 \text{ s}^{-1}$: (a) Settling $\dot{q}_1(t)$. (b) Small fluctuations in $\dot{q}_1(t)$. (c) Settling $q_3(t)$. (d) Small fluctuations in $q_3(t)$.

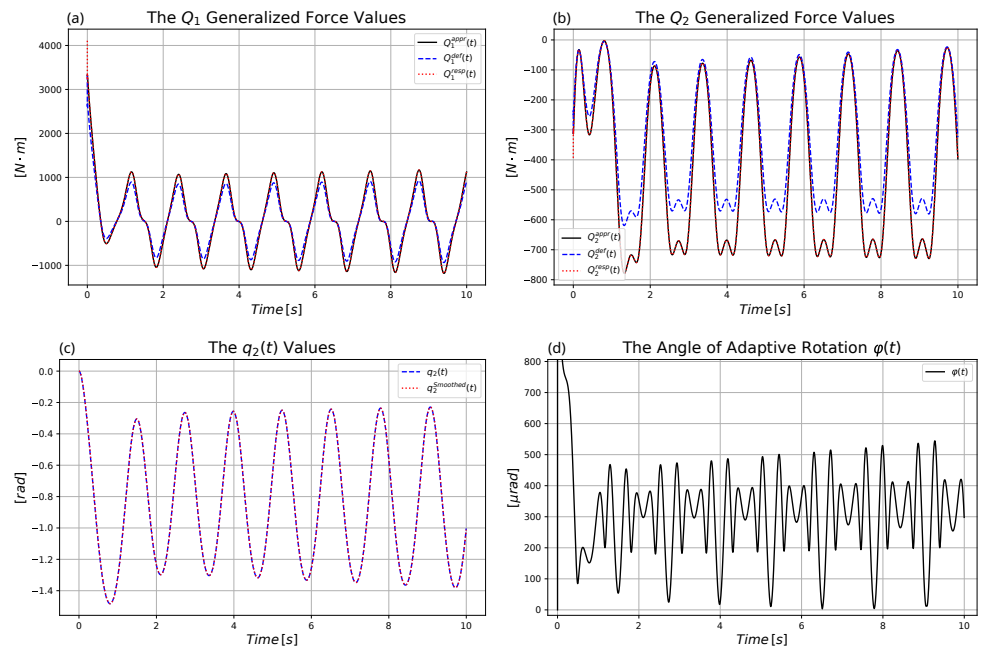


Figure 7. Results for $\Lambda_1 = \Lambda_3 = 4.0 \text{ s}^{-1}$: (a) The control force $Q_1(t)$. (b) The control force $Q_2(t)$. (c) The motion of axle $q_2(t)$. (d) Angle of the adaptive abstract rotation.

The counterparts of the above figures for $\Lambda_1 = \Lambda_3 = 8.0 \text{ s}^{-1}$ are Figures 8 and 9. They well exemplify the role of the parameters Λ_1 and Λ_3 .

In these simulations, adaptivity had a key role; without adaptive deformation the controller diverged.

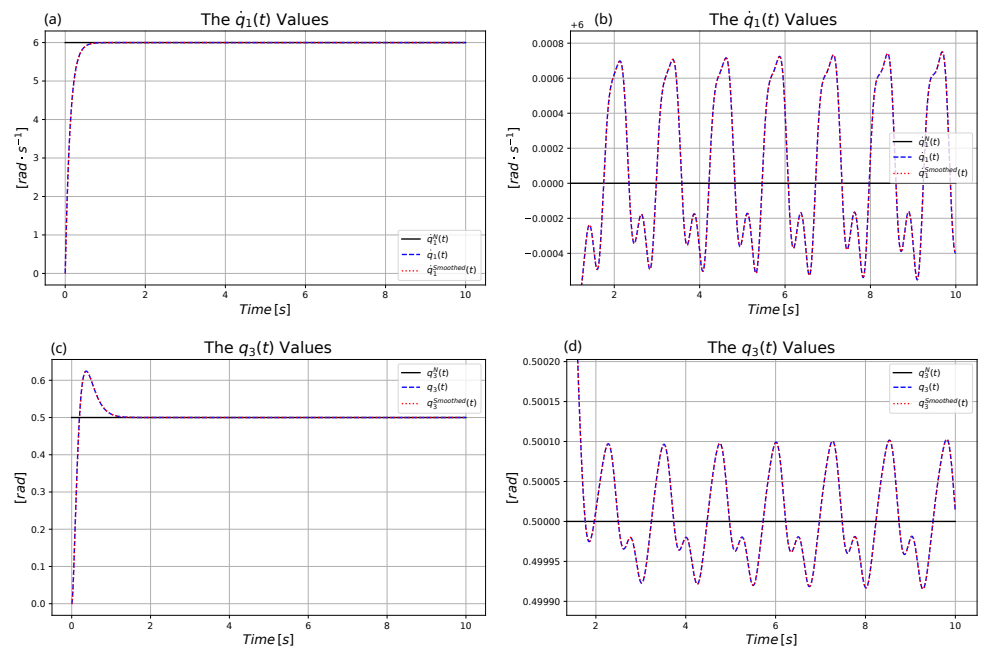


Figure 8. The nominal and realized motion for $\Lambda_1 = \Lambda_3 = 8.0 \text{ s}^{-1}$: (a) Settling $\dot{q}_1(t)$. (b) Small fluctuations in $\dot{q}_1(t)$. (c) Settling $q_3(t)$. (d) Small fluctuations in $q_3(t)$.

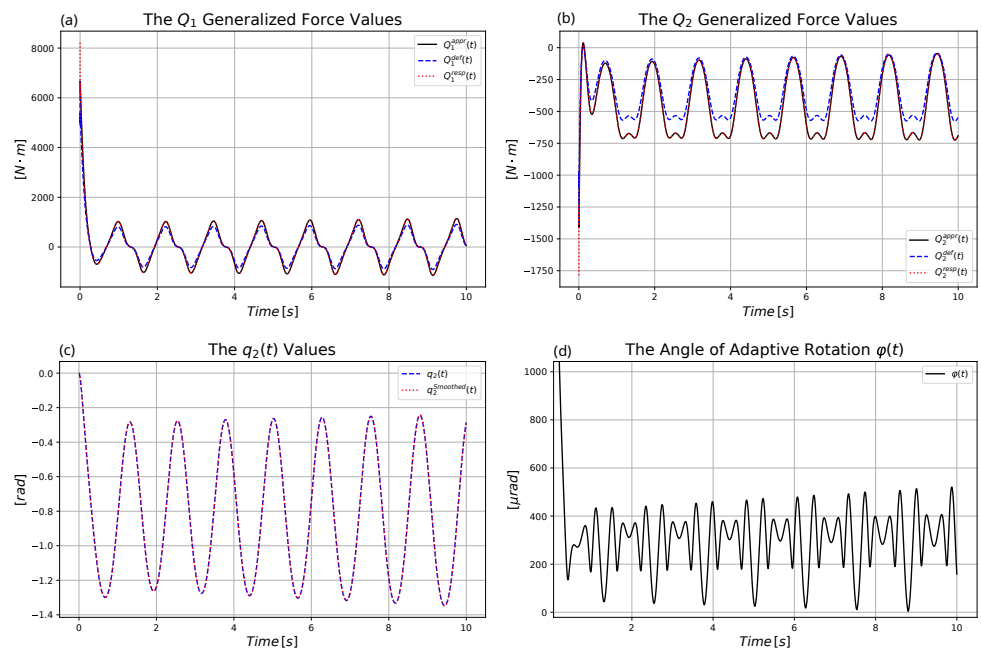


Figure 9. Results for $\Lambda_1 = \Lambda_3 = 8.0 \text{ s}^{-1}$: (a) The control force $Q_1(t)$. (b) The control force $Q_2(t)$. (c) The motion of axle $q_2(t)$. (d) Angle of the adaptive abstract rotation.

3.2.2. Simulations with Measurement Noise

In Figures 10 and 11 the same task is considered as in Section 3.2.1, but in the measurement a Gaussian noise of zero mean and $\sigma = 10^{-5}$ rad standard deviation was assumed for each axle.

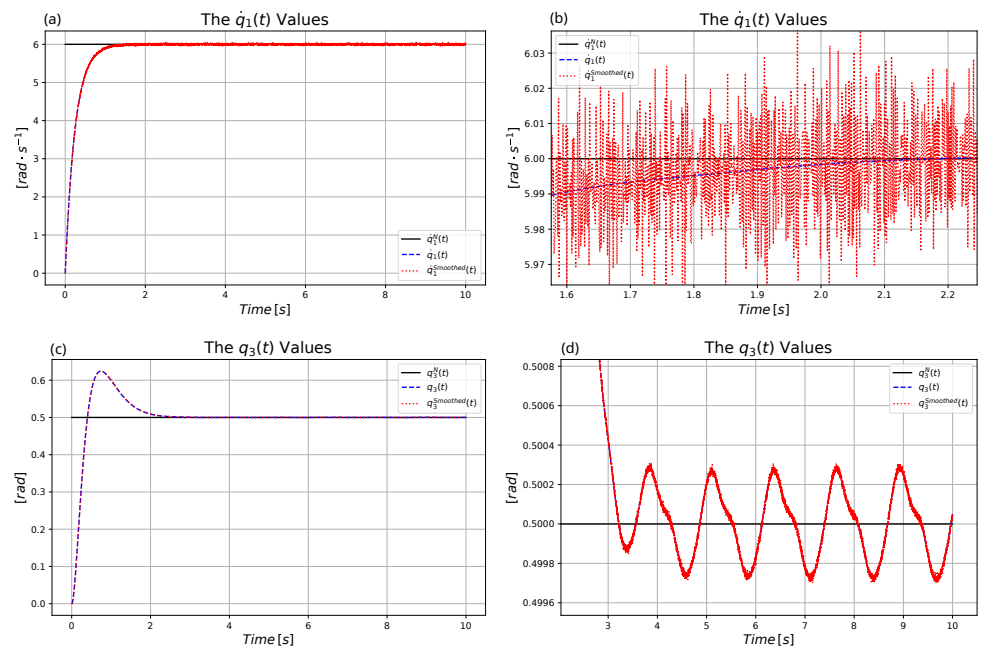


Figure 10. The nominal and realized motion under measurement noises: (a) Settling $\dot{q}_1(t)$. (b) Small fluctuations in $\dot{q}_1(t)$. (c) Settling $q_3(t)$. (d) Small fluctuations in $q_3(t)$.

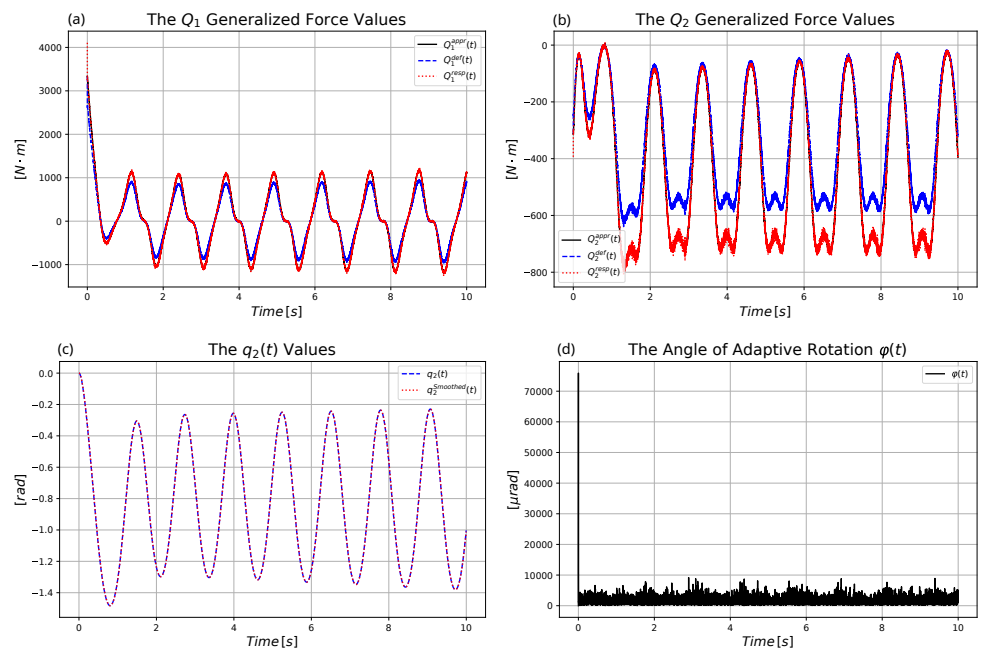


Figure 11. (a) The control force $Q_1(t)$. (b) The control force $Q_2(t)$. (c) The motion of axle $q_2(t)$. (d) Angle of the adaptive abstract rotation.

It can be concluded that the method was able to tolerate such an order of magnitude noise.

3.3. Control of Coupled Non-Linear Springs Increased to Relative Order 3

The system to be controlled is outlined in Figure 12.

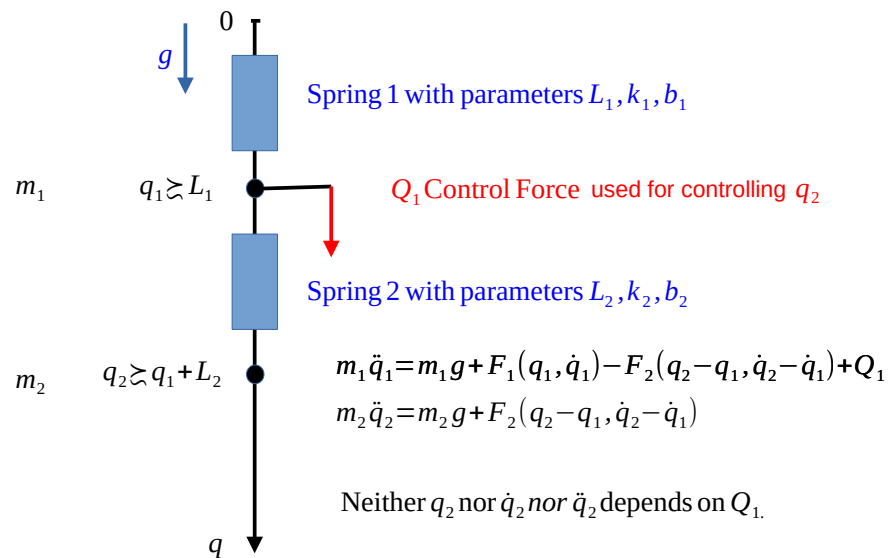


Figure 12. The kinematic structure of the coupled springs.

It is assumed that the springs have strongly non-linear model in the sense that they remain “soft” for pulling but strongly harden for compression; furthermore, they have considerable viscous friction in their motion as in Equation (11)

$$F(x, \dot{x}) \stackrel{def}{=} \begin{cases} -k(x - L) - b\dot{x} & \text{if } x \geq L, \\ -kL \ln(\frac{x}{L}) - b\dot{x} & \text{if } 0 < x < L. \end{cases} \tag{11}$$

This spring strongly hardens as its length, x , approaches 0. Later, we need the partial derivatives of this function, which are denoted as

$$F_x(x) \stackrel{def}{=} \frac{\partial F}{\partial x} = \begin{cases} -k & \text{if } x \geq L, \\ -\frac{kL}{x} & \text{if } 0 < x < L \end{cases} \tag{12}$$

$$F_y \stackrel{def}{=} \frac{\partial F}{\partial \dot{x}} = -b = \text{const.}$$

Evidently, due to the viscous friction of Spring 2, $m_2 \ddot{q}_2$ will contain \dot{q}_1 that is connected to Q_1 by the first equation:

$$m_2 \ddot{q}_2 = F_{2x}(\dot{q}_2 - \dot{q}_1) + F_{2y} \cdot (\ddot{q}_2 - \ddot{q}_1), \tag{13}$$

into which Q_1 can be substituted from the first equation of motion. Therefore, as a starting point of this task, the following three equations can be considered:

$$\ddot{q}_1 = g + \frac{1}{m_1} F_1(q_1, \dot{q}_1) - \frac{1}{m_1} F_2(q_2 - q_1, \dot{q}_2 - \dot{q}_1) + \frac{1}{m_1} Q_1, \tag{14a}$$

$$\ddot{q}_2 = g + \frac{1}{m_2} F_2(q_2 - q_1, \dot{q}_2 - \dot{q}_1), \tag{14b}$$

$$\ddot{q}_2 = \frac{1}{m_2} F_{2x}(q_2 - q_1) \cdot (\dot{q}_2 - \dot{q}_1) + \frac{1}{m_2} F_{2y} \cdot \left(\ddot{q}_2 - g - \frac{1}{m_1} F_1(q_1, \dot{q}_1) + \frac{1}{m_1} F_2(q_2 - q_1, \dot{q}_2 - \dot{q}_1) - \frac{1}{m_1} Q_1 \right). \tag{14c}$$

From this, it follows that the *relative order of our control task* is 3, because the value of $\ddot{q}_2(t)$ can be instantaneously controlled by the control force $Q_1(t)$. However, this task is different to a *normal order 3 control*, since in the normal case $\ddot{q}_2(t)$ can be set independently of $q_2(t)$, $\dot{q}_2(t)$, and $\ddot{q}_2(t)$. In our case $\ddot{q}_2(t)$ cannot be set independently of these values: the system’s dynamic model determines $\ddot{q}_2(t)$ by its lower order derivatives, and by Q_1 . This easily may lead to inconsistent kinematic requirements if the model parameters

are not exactly known and, e.g., the stiffness of the non-linear spring in our case can be divergent function of the spring’s length. Because of this, the controller’s structure outlined in Figure 13 is suggested to tackle this problem.

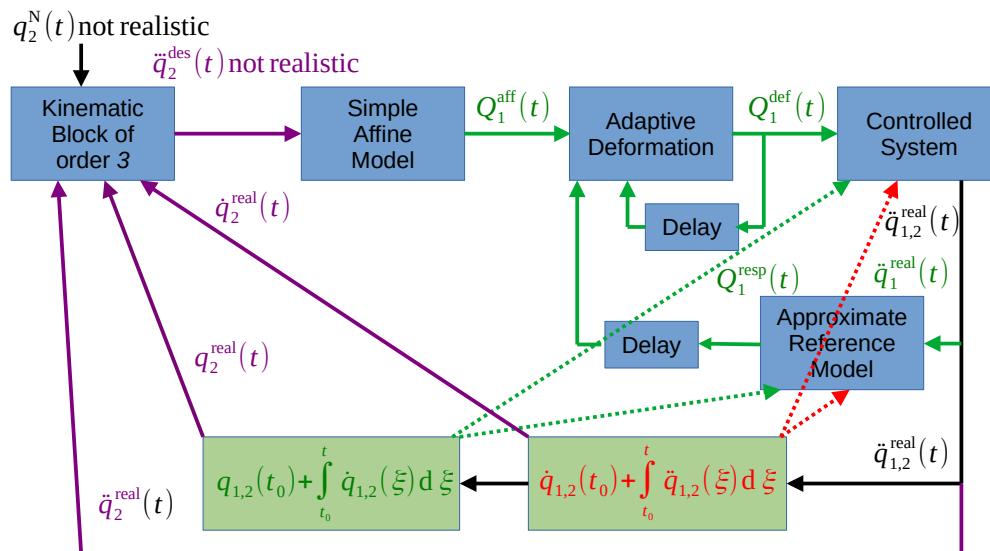


Figure 13. The control structure of the underactuated coupled springs.

In Figure 13, instead of the complicated inverse of Equation (14c) the simple affine model is used for the calculation of the reference force $Q_1^{aff}(t)$ in the box “Simple Affine Model” as

$$Q_1^{aff}(t) \approx \mathfrak{A} \ddot{q}_2^{des}(t) + \mathfrak{B} \tag{15}$$

with the parameters \mathfrak{A} and \mathfrak{B} , the effect of which, together with that of the kinematic inconsistencies, can be compensated by the adaptivity of the controller. Since $Q_1^{def}(t)$, i.e., the actually applied control force, immediately determines $\ddot{q}_1(t)$ according to the exact dynamic model parameters, the adaptation can be closed in the green loop related to Q_1^{resp} and \ddot{q}_1 according to Equation (14a) using the available approximate dynamic parameters in the box “Approximate Reference Model”. This will produce a realizable motion for $q_1(t)$ that is influenced by the not completely realistic $\ddot{q}_2^{des}(t)$ requirement. As a result the not realistic prescription will be well approximated by a realistic one. In the simulations, Euler integration happens according to Equations (14a) and (14b) using the exact dynamic model parameters.

For the kinematic prescription to vanish the tracking error, assume that we have positive constants $\lambda_k > \Lambda$, and to obtain $\ddot{q}_2(t)$ prescribe in the box “Kinematic Block of order 3” Equation (16) as

$$\left(\lambda_k + \frac{d}{dt}\right)^3 \left(\Lambda + \frac{d}{dt}\right) e_{int} \equiv 0 \tag{16}$$

Since the solution of $\left(\lambda_k + \frac{d}{dt}\right)g(t) = 0$ is $g(t) = \exp(-\lambda_k(t - t_0))g(t_0) \rightarrow 0$ as $t \rightarrow \infty$, if this strategy is realized due to adaptivity, after a while the system arrives at $\left(\Lambda + \frac{d}{dt}\right)e_{int} \equiv 0$ that yields a monotonic reduction in the integrated error.

For this system of relative order 3 the following order 4 noise filtering was applied (Equation (17)):

$$\left(\lambda_s + \frac{d}{dt}\right)^4 q_i^s(t) = \lambda_s^4 q_i^o(t) \tag{17}$$

with the initial conditions $q_i^s(t_0) = q_i(t_0) = 0$, $\dot{q}_i^s(t_0) = \dot{q}_i(t_0) = 0$, and $\ddot{q}_i^s(t_0) = \ddot{q}_i(t_0) = 0$, $\ddot{q}_i^s(t_0) = \ddot{q}_i(t_0) = 0$ with $\lambda_s = 10^3 \text{ [s}^{-1}\text{]}$. For modeling measurement noises Gaussian noise of zero mean and $\sigma = 10^{-5} \text{ m}$ was assumed.

In the simulations, the model data given in Table 3 were used.

Table 3. The kinematic and dynamic parameters of the coupled springs.

Parameter	Measurement Unit	Exact Value	Approx. Value
Length of spring 1: L_1	[m]	1.0	0.8
Length of spring 2: L_2	[m]	1.5	1.3
Mass of point 1: m_1	[kg]	1.5	2.0
Mass of point 2: m_2	[kg]	2.0	2.5
Spring stiffness 1: k_1	[N · m ⁻¹]	100.0	90.0
Spring stiffness 2: k_2	[N · m ⁻¹]	200.0	190.0
Gravitational acceleration: g	[m · s ⁻²]	9.81	9.81
Viscous damping 1: b_1	[N · s · m ⁻¹]	2.5	2.0
Viscous damping 2: b_2	[N · s · m ⁻¹]	3.0	2.5
Affine parameter 1: \mathfrak{A}	[N · s ³ · m ⁻¹]	Not applicable	various
Affine parameter 2: \mathfrak{B}	[N]	Not applicable	−15.0

For setting the parameters it was assumed that the gravitational acceleration is known, but the other model data should have considerable approximation errors as underestimated “zero force lengths” for the springs, overestimated masses, underestimated spring stiffness values, and viscous friction terms.

For the spring system, the numerical data given in Table 4 were used with a deformed and shifted sinusoidal nominal trajectory determined by Equation (18) as

$$q_2^N(t) = \tanh\left(\frac{t}{T}\right) A_o \tanh(A_i \sin \Omega t) + S \tag{18}$$

In this manner, more complex motions can be considered than the simple sinusoidal ones. Furthermore, the “rule” that it is not expedient to apply an initial shock to a non-linear system is taken into consideration too. (Since linear time-invariant systems have only additional transients, in their case arbitrary initial shocks, such as abrupt jumps in the nominal trajectory to be tracked, can be applied without significant consequences). For the simulations the data given in Table 4 were used.

Table 4. Controller and simulation data for the coupled springs.

Parameter	Measurement Unit	Value
Digital time resolution: δt	[s]	10^{-3}
Noise filtering parameter λ_s	[s ⁻¹]	10^3
Adaptive interp. param. λ_a	[nondimensional]	0.9, 0.05
Trajectory tracking parameter Λ	[s ⁻¹]	4.0
Trajectory tracking parameter λ_k	[s ⁻¹]	12.0
Norm of augmented vectors R_a	[N]	10^{-6}
σ of Gaussian noise	[m]	0 and 10^{-6}
Nominal trajectory rise time T	[s]	3.0
Nominal trajectory amplitude A_o	[m]	$0.2 \cdot (L_1 + L_2)$ (exact)
Nominal trajectory deformation factor A_i	[nondimensional]	2.0
Nominal trajectory circular frequency Ω	[s ⁻¹]	2.0
Nominal trajectory shift S	[m]	$(L_1 + L_2)$ (exact)

3.3.1. Simulations for the Affine Model without Measurement Noise

At first, the role of the adaptive deformation in using the simple affine model is illustrated. In Figure 14, it can be observed that without the adaptation a long-lasting fluctuation in the control force and in the motion of coordinate q_1 was generated.

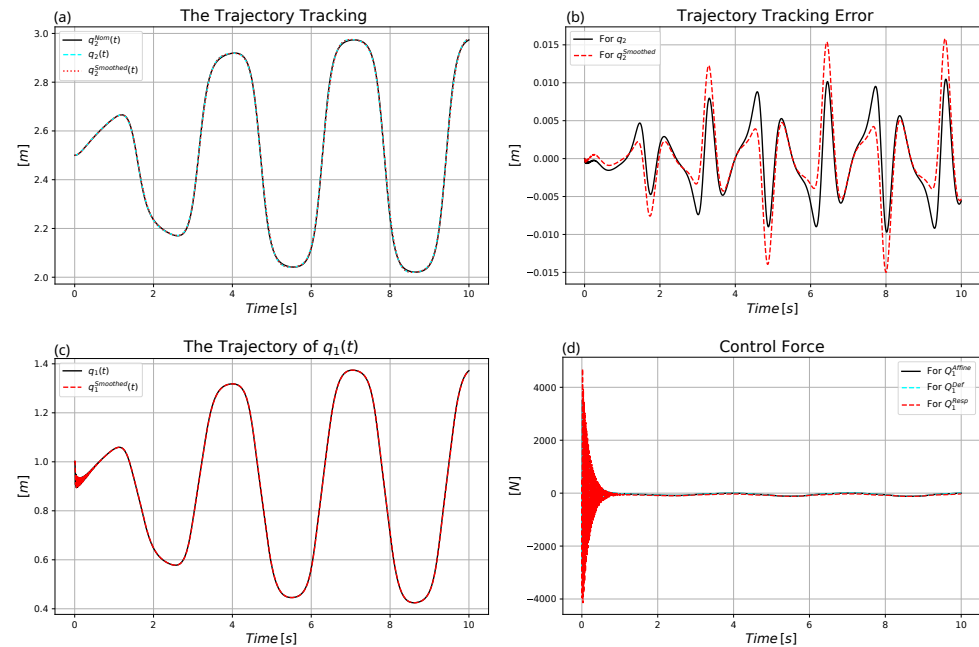


Figure 14. Control of the affine model with $\mathfrak{A} = 7.0 \text{ [N} \cdot \text{s}^3 \cdot \text{m}^{-1}]$ without adaptivity: (a) Trajectory tracking. (b) Trajectory tracking error. (c) The motion of mass point 1. (d) The control force.

On the basis of Figures 14–17 the following observations can be performed:

1. While the tracking error remained in the same range, the illusion of the MRAC control, i.e., that on the basis of the kinematic prescriptions the dynamics of the affine model was controlled was well provided by the solution. The affine model was used by the external kinematic loop for the computation of the necessary control force, and precise trajectory tracking was achieved. The affine model's force need was approximately in the range $[-120, -30] \text{ N}$ following the transient phase, while the actual control force varied within the range $[-120, 5] \text{ N}$.
2. Due to the adaptivity the duration of the initial “transient swinging phase” of the control force was considerably reduced.
3. The duration of the initial transient swinging in the position of mass point 1 was considerably reduced due to the adaptivity.
4. Furthermore, the application of adaptivity considerably reduced the amplitude of the control force in the initial transient phase of the motion from the range $[-4000, 4500] \text{ N}$ to $[-3000, 2500] \text{ N}$.

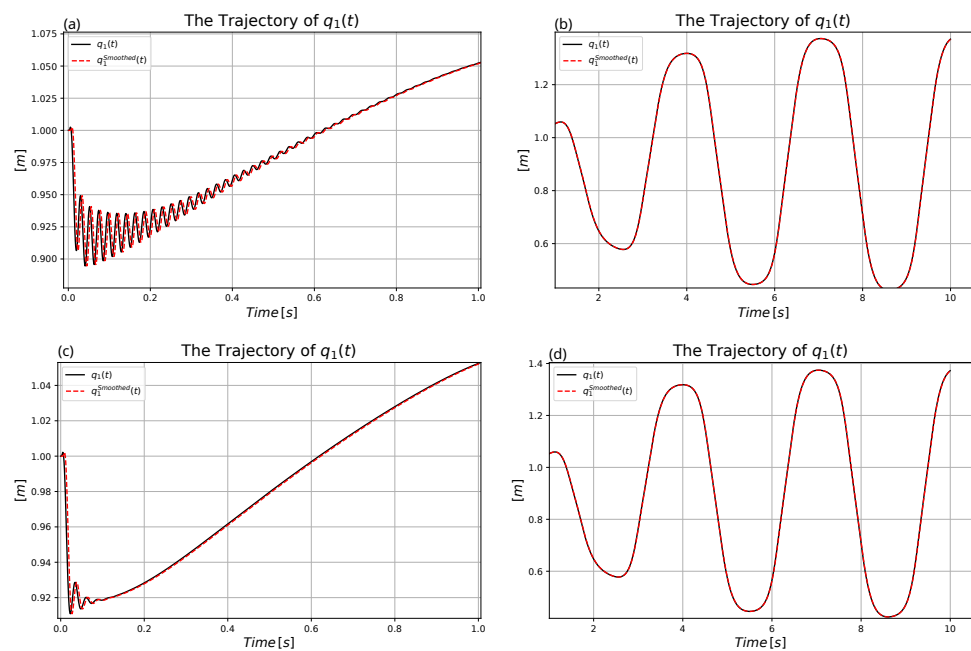


Figure 15. Comparison of the motion of q_1 for the adaptive and the non-adaptive control for $\mathfrak{A} = 7.0 \text{ [N} \cdot \text{s}^3 \cdot \text{m}^{-1}]$. (a) Non-adaptive motion of q_1 in the first second. (b) Non-adaptive motion of q_1 in the rest of the trajectory. (c) Adaptive motion of q_1 in the first second. (d) Adaptive motion of q_1 in the rest of the trajectory.

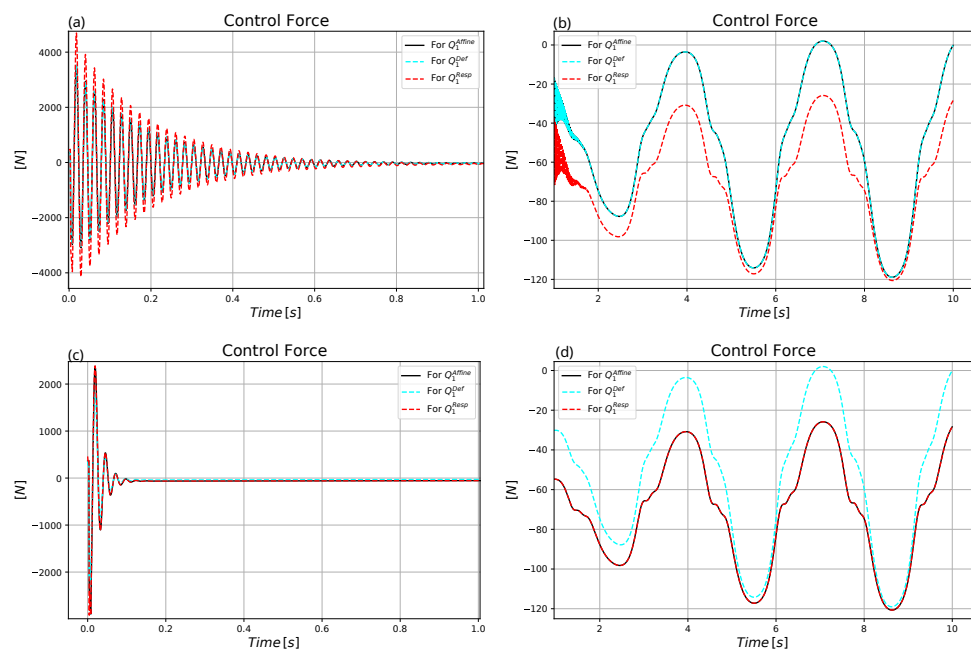


Figure 16. Comparison of the control force Q_1 for the adaptive and the non-adaptive control for $\mathfrak{A} = 7.0 \text{ [N} \cdot \text{s}^3 \cdot \text{m}^{-1}]$. (a) Non-adaptive motion in the first second. (b) Non-adaptive motion in the rest of the trajectory. (c) Adaptive motion in the first second. (d) Adaptive motion in the rest of the trajectory.

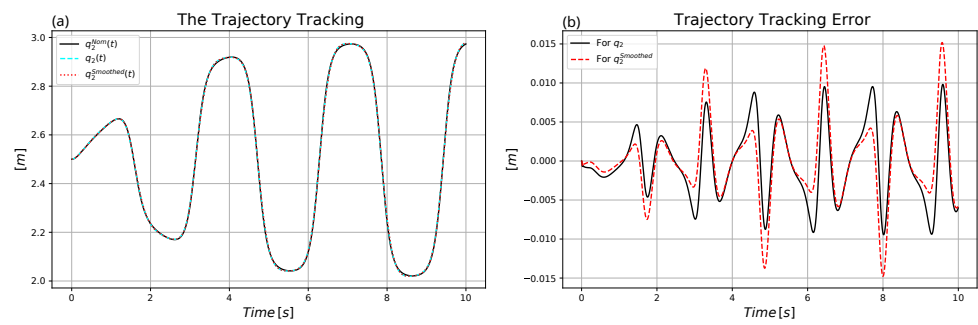


Figure 17. Control of the affine model with $\mathfrak{A} = 7.0 \text{ [N} \cdot \text{s}^3 \cdot \text{m}^{-1}]$ and adaptivity: (a) Trajectory tracking. (b) Trajectory tracking error.

The next figures (Figures 18–20) reveal the results for the $\mathfrak{A} = 5.0 \text{ [N} \cdot \text{s}^3 \cdot \text{m}^{-1}]$ affine parameter. The same observations can be made in the case of these results as in the case of the set belonging to $\mathfrak{A} = 7.0 \text{ [N} \cdot \text{s}^3 \cdot \text{m}^{-1}]$.

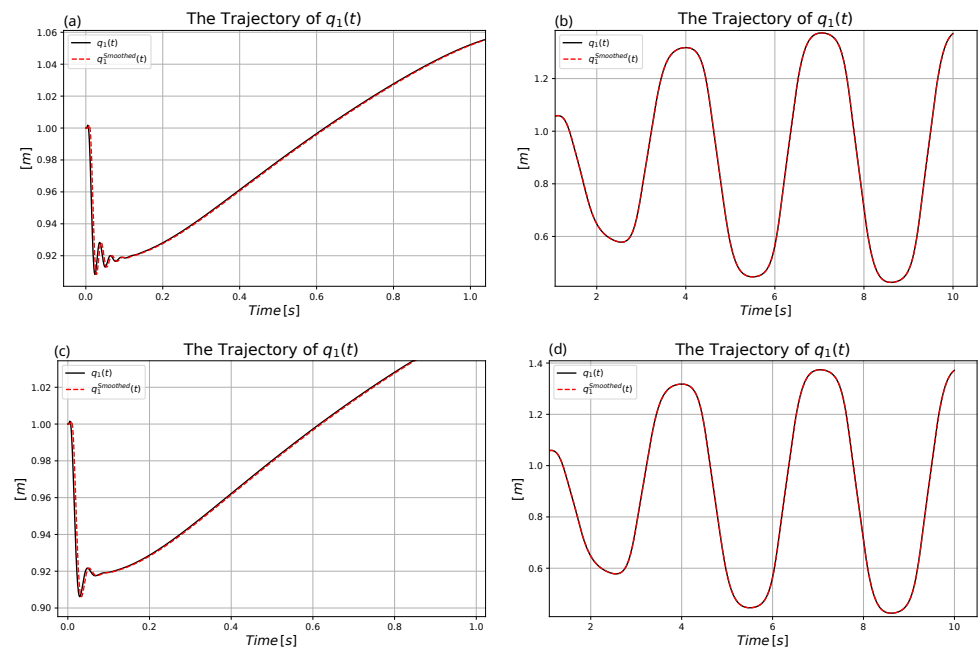


Figure 18. Comparison of the motion of q_1 for the adaptive and the non-adaptive control for $\mathfrak{A} = 5.0 \text{ [N} \cdot \text{s}^3 \cdot \text{m}^{-1}]$. (a) Non-adaptive motion of q_1 in the first second. (b) Non-adaptive motion of q_1 in the rest of the trajectory. (c) Adaptive motion of q_1 in the first second. (d) Adaptive motion of q_1 in the rest of the trajectory.

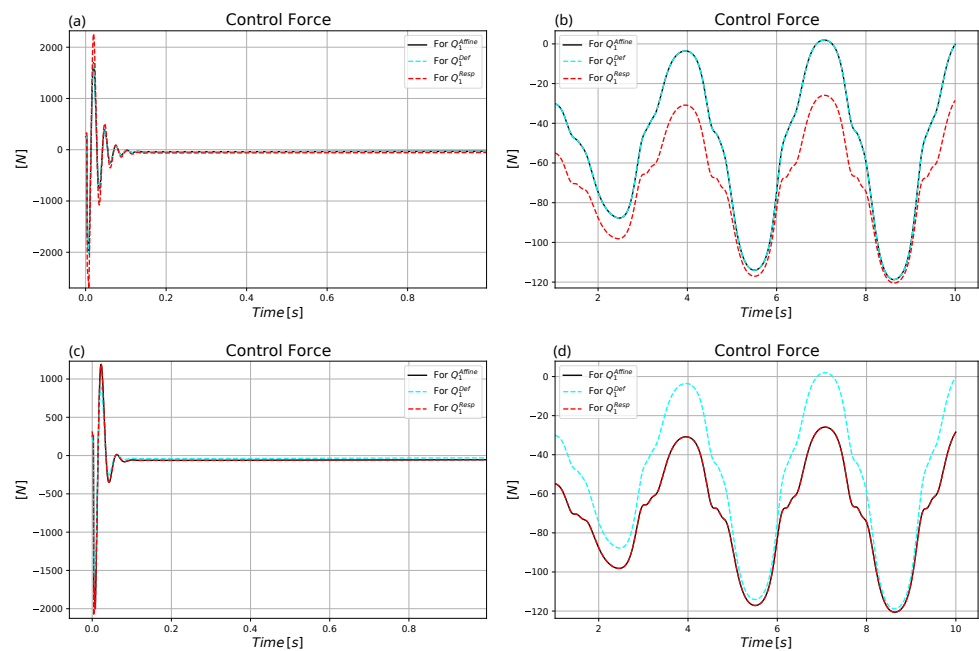


Figure 19. Comparison of the control force Q_1 for the adaptive and the non-adaptive control for $\mathfrak{A} = 5.0 \text{ [N} \cdot \text{s}^3 \cdot \text{m}^{-1}]$. (a) Non-adaptive motion in the first second. (b) Non-adaptive motion in the rest of the trajectory. (c) Adaptive motion in the first second. (d) Adaptive motion in the rest of the trajectory.

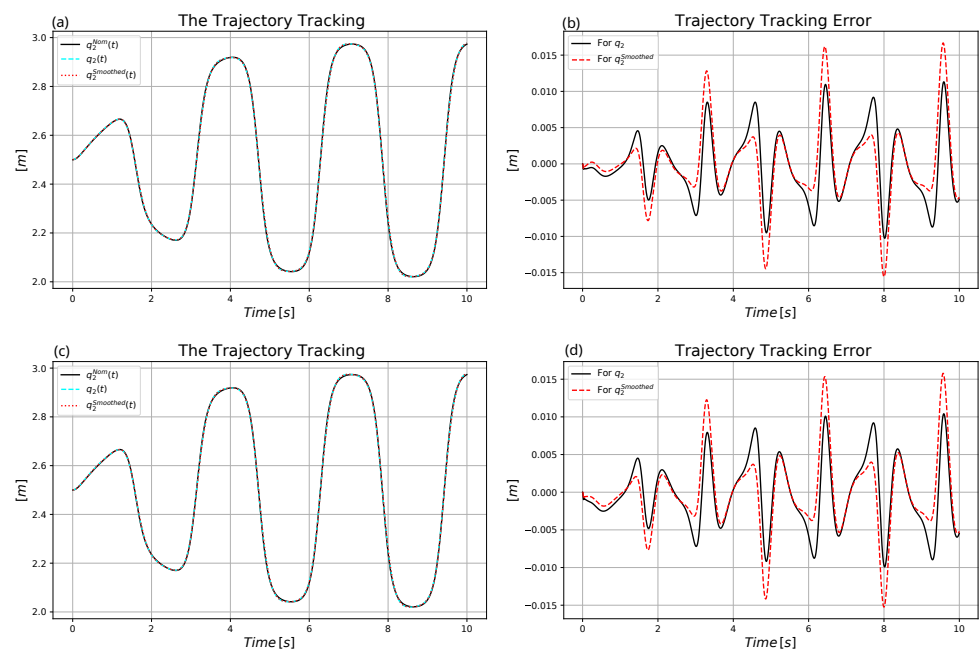


Figure 20. Control of the affine model with $\mathfrak{A} = 5.0 \text{ [N} \cdot \text{s}^3 \cdot \text{m}^{-1}]$ (a) Non-adaptive trajectory tracking. (b) Non-adaptive trajectory tracking error. (c) Adaptive trajectory tracking. (d) Adaptive trajectory tracking error.

In the following section, the effects of an extremely low value, $\mathfrak{A} = 0.4 \text{ s}^3 \cdot \text{m}^{-1}$ are investigated. Figures 21–23 reveal that in this case, when very drastic inconsistency is present between the affine model and the realistic one, the adaptive controller produces more hectic variation of coordinate $q_1(t)$ and in the control force. However, the MRAC illusion is well maintained, since the affine and the response forces are very close to each

other, and considerably differ from the actual control (i.e., the deformed) forces. In this case the precision of the trajectory tracking is a little bit improved.

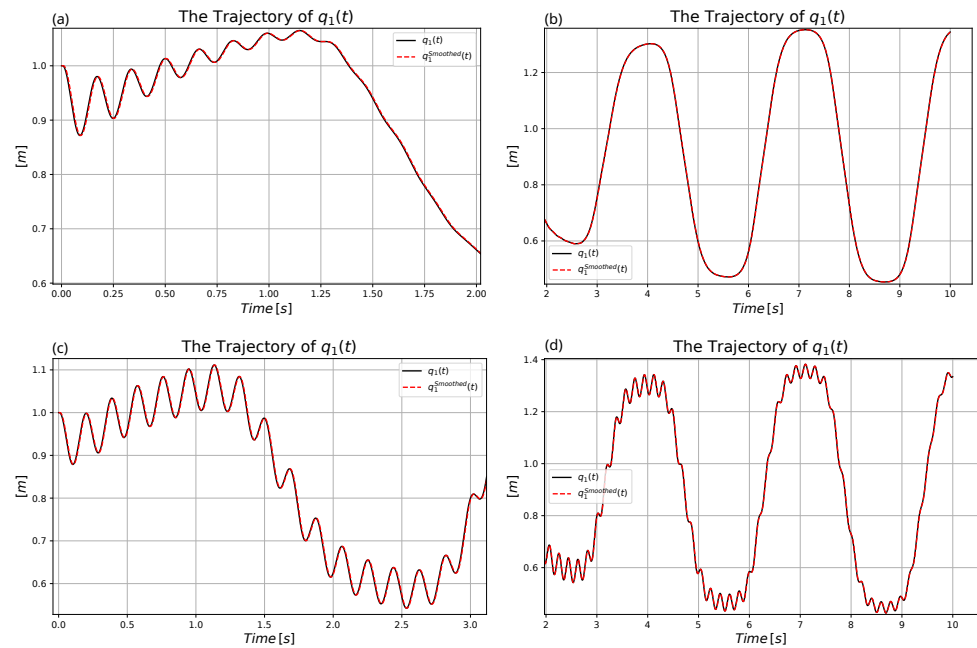


Figure 21. Comparison of the motion of q_1 for the adaptive and the non-adaptive control for $\mathfrak{A} = 0.4 \text{ [N} \cdot \text{s}^3 \cdot \text{m}^{-1}]$ (a) Non-adaptive motion of q_1 in the first two seconds. (b) Non-adaptive motion of q_1 in the rest of the trajectory. (c) Adaptive motion of q_1 in the first three seconds. (d) Adaptive motion of q_1 in the rest of the trajectory.

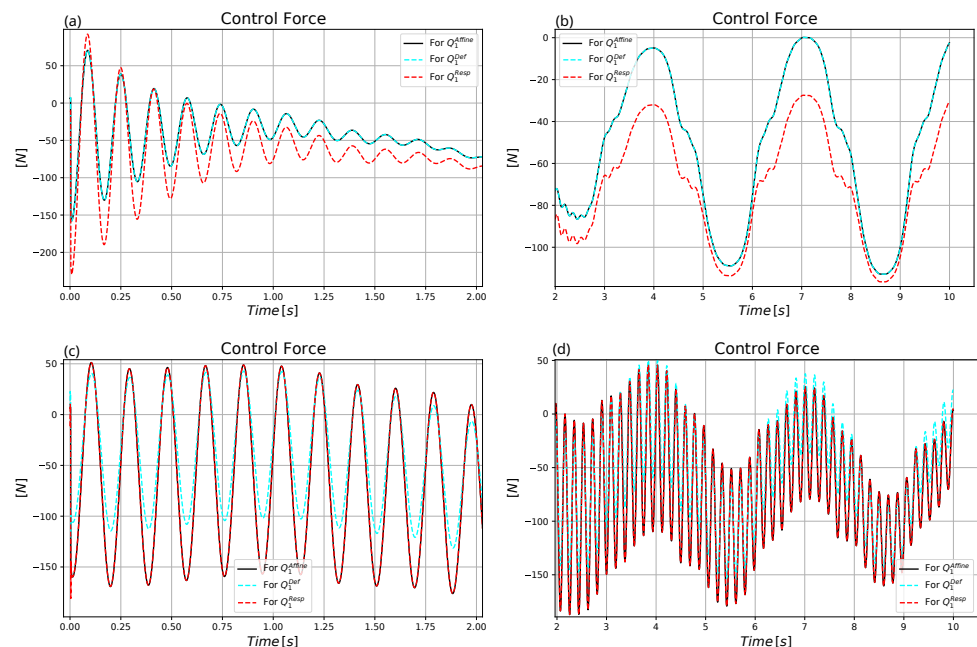


Figure 22. Comparison of the control force Q_1 for the adaptive and the non-adaptive control for $\mathfrak{A} = 0.4 \text{ [N} \cdot \text{s}^3 \cdot \text{m}^{-1}]$ (a) Non-adaptive motion in the first two seconds. (b) Non-adaptive motion in the rest of the trajectory. (c) Adaptive motion in the first two seconds. (d) Adaptive motion in the rest of the trajectory.

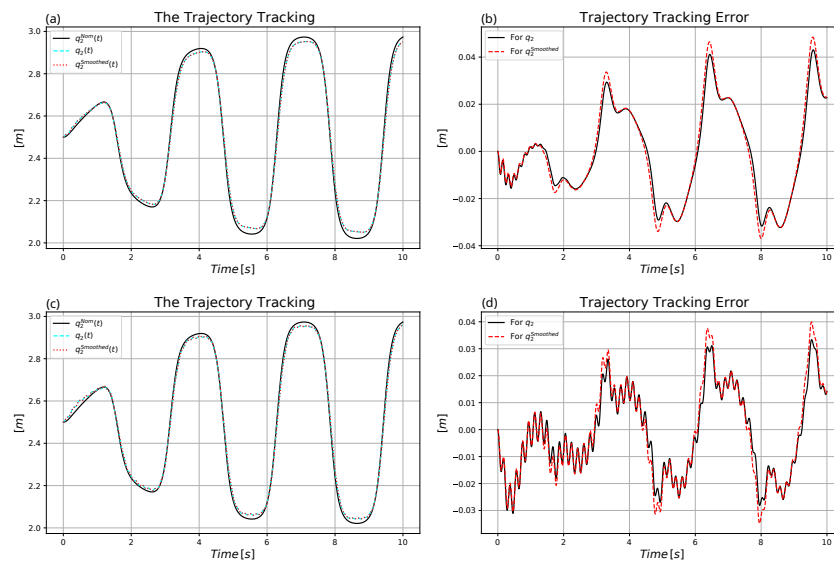


Figure 23. Control of the affine model with $\mathfrak{A} = 0.4 \text{ [N} \cdot \text{s}^3 \cdot \text{m}^{-1}]$ (a) Non-adaptive trajectory tracking. (b) Non-adaptive trajectory tracking error. (c) Adaptive trajectory tracking. (d) Adaptive trajectory tracking error.

As it can be expected from the dynamic model, the necessary control forces mainly depend on the amplitude of the nominal motion that directly concerns the spring dilatation/compression values, and the time-derivatives of the coordinates that generate the friction forces. The affine parameter \mathfrak{A} mainly determines the duration of the initial oscillating phase. It can be noted, too, that in harmony with the expectation for the “*approximately differentially direction keeping*” response function, for $\mathfrak{A} < 0$ and too small $\mathfrak{A} > 0$ the adaptive controller became divergent.

3.3.2. Simulations for the Affine Model with Measurement Noise

In this case, non-adaptive and adaptive simulations were made for $\mathfrak{A} = 7.0 \text{ [N} \cdot \text{s}^3 \cdot \text{m}^{-1}]$. Figures 24 and 25 reveal the chaotic fluctuation in the control force that does not completely destroy adaptivity.

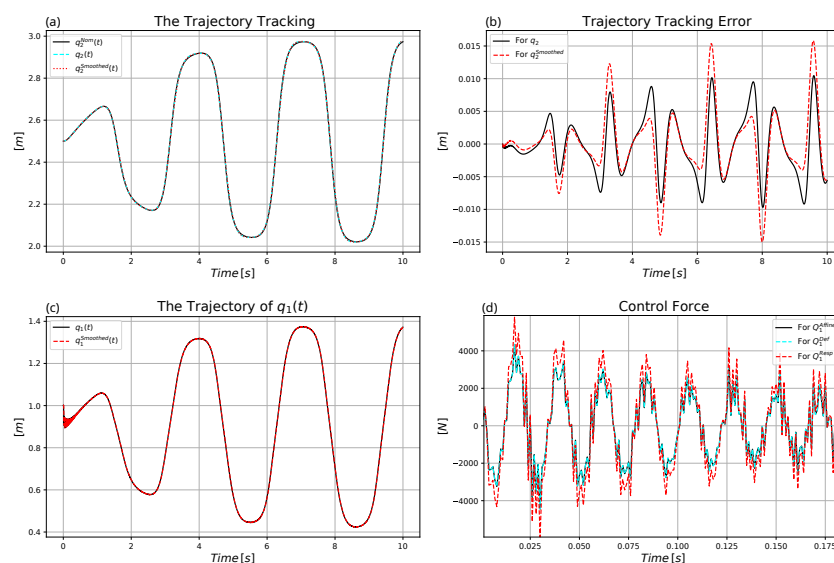


Figure 24. Control of the affine model with $\mathfrak{A} = 7.0 \text{ [N} \cdot \text{s}^3 \cdot \text{m}^{-1}]$ without adaptivity under measurement noises: (a) Trajectory tracking. (b) Trajectory tracking error. (c) The motion of mass point 1. (d) The control force (zoomed in excerpt).

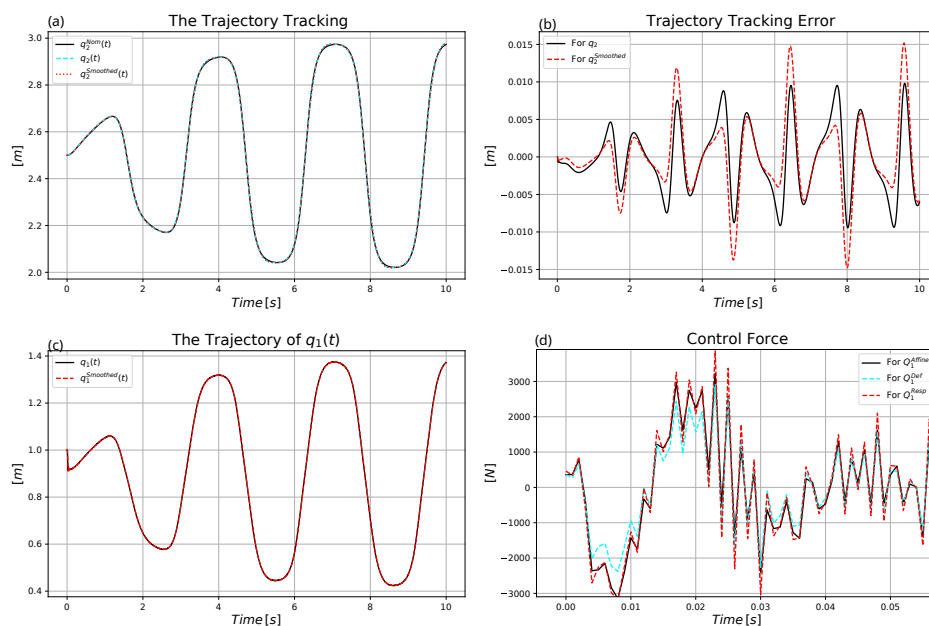


Figure 25. Control of the affine model with $\mathfrak{A} = 7.0 \text{ [N} \cdot \text{s}^3 \cdot \text{m}^{-1}]$ with adaptivity under measurement noises: (a) Trajectory tracking. (b) Trajectory tracking error. (c) The motion of mass point 1. (d) The control force (zoomed in excerpt).

3.3.3. Simulations for the Complex Order 3 Model without Measurement Noise

For comparison the original version of the FPI-based MRAC controller for fully actuated systems (Figure 3) has been modified for the order 3 underactuated version in Figure 26. In this case, the inverse of Equation (14c), i.e., Equation (19) is used in the boxes “Complex Reference Model” with the available approximate model parameters.

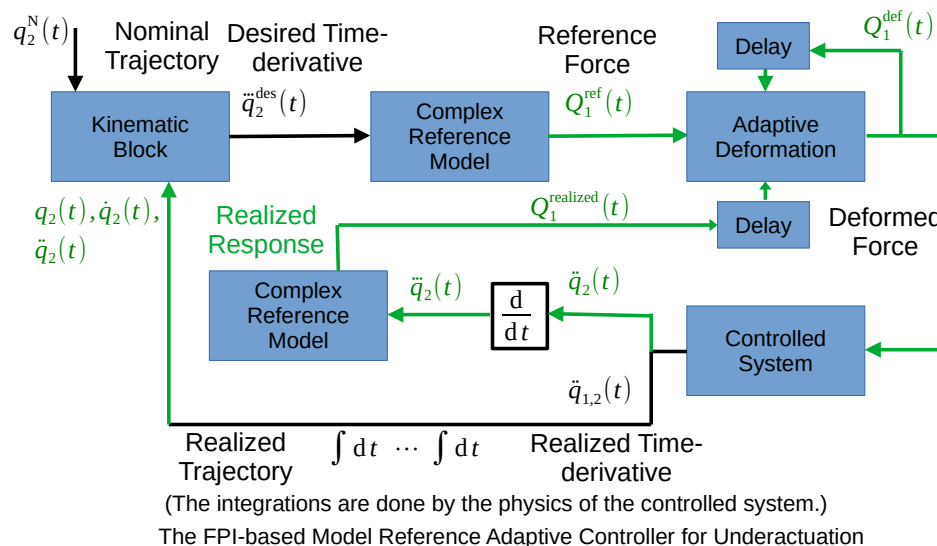


Figure 26. The control structure of the underactuated coupled springs using the complex order 3 model: the input of the “Complex Reference Model” corresponds to the function in Equation (19). For the sake of clarity the figure does not contain each input.

$$Q_1 = \frac{-m_1}{F_{2y}} \left[m_2 \ddot{q}_2 - F_{2x}(q_2 - q_1)(\dot{q}_2 - \dot{q}_1) - F_{2y} \left\{ \ddot{q}_2 - g - \frac{1}{m_1} F_1(q_1, \dot{q}_1) + \frac{1}{m_1} F_2(q_2 - q_1, \dot{q}_2 - \dot{q}_1) \right\} \right] . \tag{19}$$

In the simulations for the input of Equation (19) the noise-filtered estimations of q_1 , q_2 , \dot{q}_1 , \dot{q}_2 , and \ddot{q}_2 are used. The Julia language code excerpt of this function is given below

```
function Q_3rd0rdModel(q2_pppDes, q1, q2, q1_p, q2_p, q2_pp)
    local casual
    casual=m2a*q2_pppDes-F2xa(q2-q1)*(q2_p-q1_p)
    casual-=F2ya*(q2_pp-ga-F1a(q1, q1_p)/m1a+F2a(q2-q1, q2_p-q1_p)/m1a)
    return -m1a*casual/F2ya
end
```

in which q_1 and q_2 stand for q_1 and q_2 , $q1_p$ and $q2_p$ is in the role of \dot{q}_1 and \dot{q}_2 , and $q2_pp$ represents \ddot{q}_2 , $m1a$, $m2a$, and ga denote the approximate parameter values of m_1 , m_2 , and g , $F2xa$ and $F2ya$ correspond to the functions F_{2x} and F_{2y} in Equation (12) with the approximate model parameters. In a similar manner, the functions $F1a$ and $F2a$ are the counterparts of the functions in Equation (11).

The following conclusions can be made regarding the results of the noise-free simulations:

1. The tracking precision for the simple affine reference model with $\mathfrak{A} = 7.0 \text{ [N} \cdot \text{s}^3 \cdot \text{m}^{-1}]$ is in the same range as in the case of the complicated order 3 model (compare Figures 14, 17 and 27).
2. The actually exerted forces are essentially the same that is determined by the desired motion, observable differences appear only in the “MRAC illusions” provided by the different solutions (compare Figures 16 and 28).
3. By the use of the affine model the initial transients were successfully reduced (compare Figures 15 and 29).

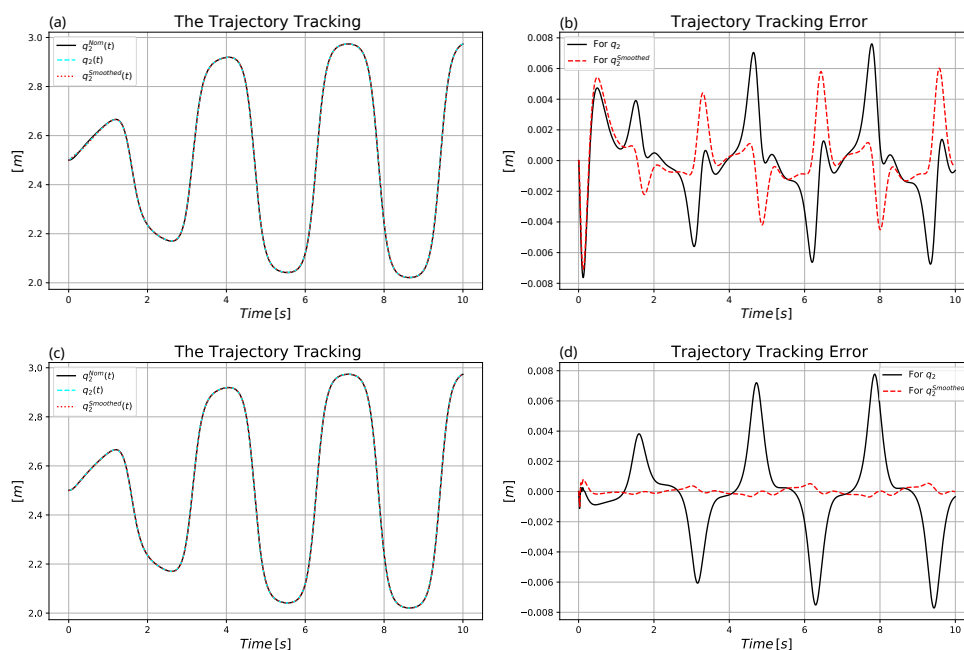


Figure 27. Control of the complex model without measurement noises: (a) Non-adaptive trajectory tracking. (b) Non-adaptive trajectory tracking error. (c) Adaptive trajectory tracking. (d) Adaptive trajectory tracking error.

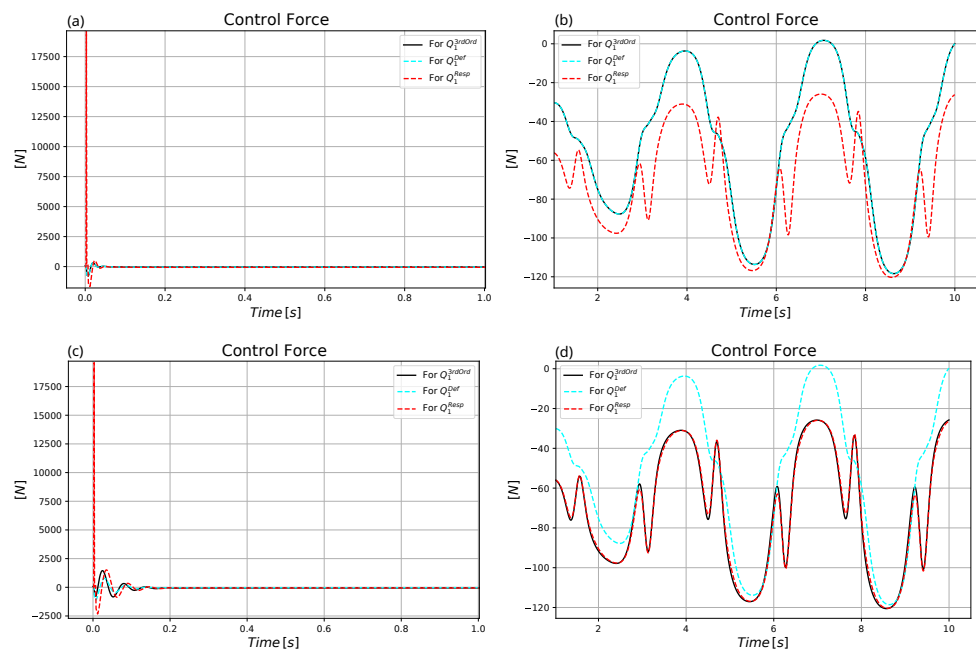


Figure 28. Comparison of the control force Q_1 for the adaptive and the non-adaptive control for the complex model without measurement noises. (a) Non-adaptive motion in the first second. (b) Non-adaptive motion in the rest of the trajectory. (c) Adaptive motion in the first second. (d) Adaptive motion in the rest of the trajectory.

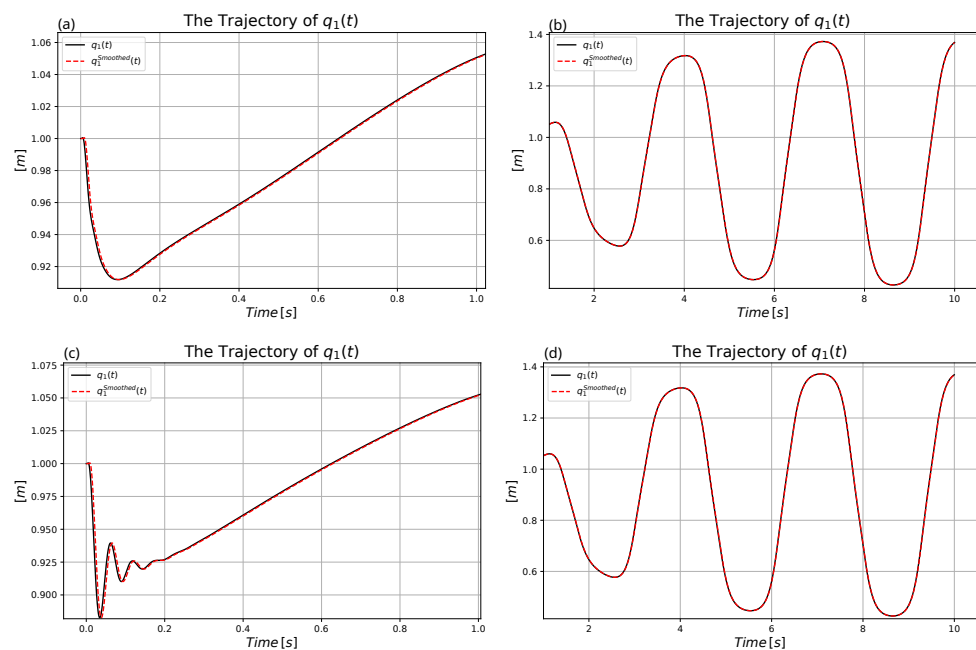


Figure 29. Comparison of the motion of q_1 for the adaptive and the non-adaptive control for the complex model without measurement noises (a) Non-adaptive motion of q_1 in the first second. (b) Non-adaptive motion of q_1 in the rest of the trajectory. (c) Adaptive motion of q_1 in the first second. (d) Adaptive motion of q_1 in the rest of the trajectory.

3.3.4. Simulations for the Complex Order 3 Model with Measurement Noise

Certain results with measurement noises are given in Figure 30. The comparison with Figure 25 reveals that the attempt of feeding back high order derivatives and using them in the adaptive iteration makes the method very noise-sensitive. Though the exerted (deformed) control forces are not too high, in the case of the complex model using various

derivatives as the input does not provide some clear “MRAC illusion”, since the “response force” has huge noise. However, in the case of the simple affine model with lower order adaptive feedback this function can be identified in the computational results.

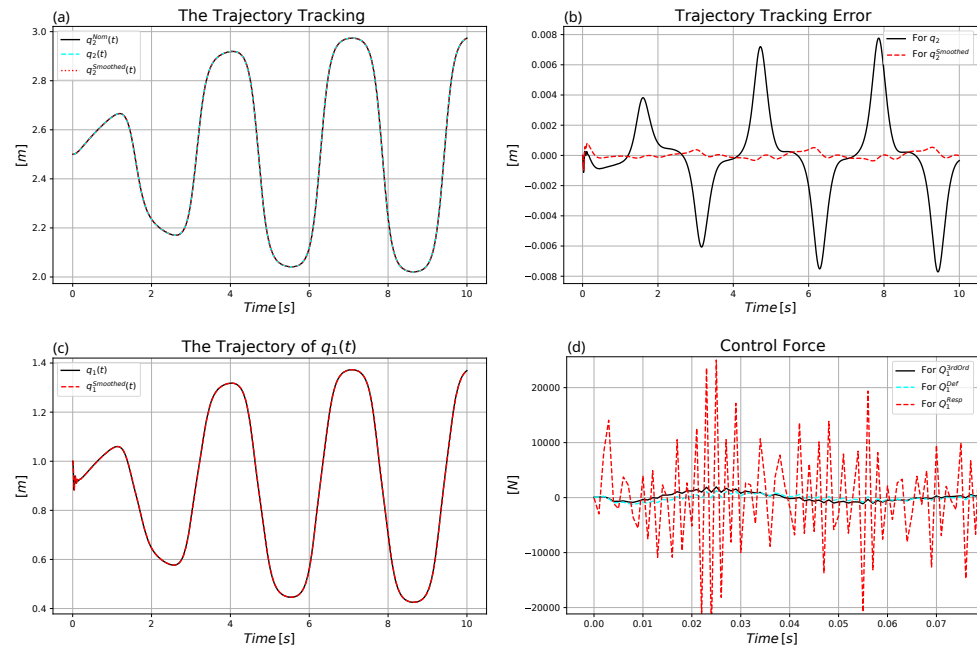


Figure 30. Control of the complex model with adaptivity under measurement noises: (a) Trajectory tracking. (b) Trajectory tracking error. (c) The motion of mass point 1. (d) The control force (zoomed in excerpt).

3.4. Summary of the Innovation

In this paper, the history of the formation of the here suggested control method was outlined step-by-step. It was shown how the FPIAC controller had been transformed into the FPI-based MRAC controller for controlling *fully actuated systems*. The present innovation is the modification of this latter method to control *underactuated systems* by the application of the adaptive deformation algorithm to *only a reduced number of the generalized coordinates of the controlled system*.

Furthermore, the increased relative order task allowed the use of a simple primitive affine model with lower order adaptive feedback instead of the calculation of the complicated model terms on the basis of approximate model parameters. In this manner, the method produced shortened initial swinging and considerably reduced noise sensitivity in comparison with the original higher order approach.

The primitive affine model is so simple that it can be realized in an embedded system. Together with the approximate model parameters used in the computations it provided a fictive “reference system” by which the inconsistencies between the high relative order kinematic design and the dynamic properties of the model were eliminated or evaded.

4. Conclusions

This paper systematically investigated the FPIAC method to adaptively control approximately modeled underactuated systems. In the suggested solution, the iteration that yielded the appropriate control signal was moved from the space of the time-derivatives of the generalized coordinates to the space of the generalized forces as in the case of the FPI-based MRAC controllers developed for fully actuated systems. However, the loop of adaptive deformation was applied only for the generalized coordinates that played independent roles in the control of the underactuated systems.

It was shown that when the underactuation causes an increase in the relative order of the control, the kinematic specifications separated from the dynamic model may be incompatible with the physical capabilities of the controlled system. This discrepancy was resolved by the application of further convenient simplification. Instead, making an attempt to estimate the higher order derivative of interest by the use of Lie derivatives and the available approximate system model a *simple affine* model part was introduced. The integrated effects of these approximations were compensated by the adaptive deformation.

Two typical examples were investigated by Julia language-based simulations, when the underactuation was not accompanied by an increase in the relative order of the controller and when the relative order was increased. For the first case, the dynamic model of a 3-degree-of-freedom robot arm was considered with a corrupted drive. For the second case, dynamically coupled strongly non-linear springs were modeled.

Though it can be expected that due to the “not conventional feedback terms”, the system must be noise sensitive, it has been shown by the simulations that simple low pass filters can be incorporated into the controller so that it remains convergent under little standard deviation of the noise that appears in the measurement of the generalized coordinates’ values.

In addition to potential noise sensitivity, the main drawback of the method is that during one digital control step only one step of the adaptive deformation can be completed. Since the speed of convergence depends on the model and the actual systems parameters according to Equation (4), on the parameter α in Equation (9) or the interpolation parameter λ_a used in [44], the general possibility to improve accuracy is the reduction in digital cycle time. In this manner, the number of the iterative steps made during unit time can be increased.

Author Contributions: Individual contributions by the Authors: Conceptualization, A.A.; Formal analysis, J.K.T.; Methodology, A.A.; Software, A.A.; Validation, J.K.T.; Writing—original draft, J.K.T. All authors have read and agreed to the published version of the manuscript.

Funding: This research was supported by the National Research, Development and Innovation Office (NKFIH) under OTKA Grant Agreement No. K 135512. We also acknowledge the support by the Doctoral School of Applied Informatics and Applied Mathematics of Óbuda University.

Data Availability Statement: Not applicable.

Conflicts of Interest: The authors declare no conflict of interest.

References

1. Armstrong, B.; Khatib, O.; Burdick, J. The Explicit Dynamic Model and Inertial Parameters of the PUMA 560 Arm. In Proceedings of the IEEE Conference on Robotics and Automation 1986, San Francisco, CA, USA, 7–10 April 1986; pp. 510–518. [\[CrossRef\]](#)
2. Sciavicco, L.; Siciliano, B. *Modeling and Control of Robot Manipulators*; McGraw-Hill: New York, NY, USA, 1996. [\[CrossRef\]](#)
3. Richalet, J.; Rault, A.; Testud, J.; Papon, J. Model predictive heuristic control: Applications to industrial processes. *Automatica* **1978**, *14*, 413–428. [\[CrossRef\]](#)
4. Clarke, D.; Mohtadi, C.; Tuffs, P. Generalized Predictive Control—Part I. The basic algorithm. *Automatica* **1987**, *23*, 137–148. [\[CrossRef\]](#)
5. Clarke, D.; Mohtadi, C.; Tuffs, P. Generalized Predictive Control—Part II. Extensions and interpretations. *Automatica* **1987**, *23*, 149–160. [\[CrossRef\]](#)
6. Corke, P.; Armstrong-Helouvry, B. A search for consensus among model parameters reported for the PUMA 560 robot. In Proceedings of the 1994 IEEE International Conference on Robotics and Automation, San Diego, CA, USA, 8–13 May 1994; Volume 2, pp. 1608–1613. [\[CrossRef\]](#)
7. Slotine, J.; Li, W. *Applied Nonlinear Control*; Prentice-Hall International, Ed.; Prentice-Hall: Hoboken, NJ, USA, 1991.
8. Kamnik, R.; Matko, D.; Bajd, T. Application of Model Reference Adaptive Control to Industrial Robot Impedance Control. *J. Intell. Robot. Syst.* **1998**, *22*, 153–163. [\[CrossRef\]](#)
9. Nguyen, C.; Antrazi, S.; Zhou, Z.L.; Campbell, C., Jr. Adaptive Control of a Stewart Platform-based Manipulator. *J. Robot. Syst.* **1993**, *10*, 657–687. [\[CrossRef\]](#)
10. Nguyen, N.T. Lyapunov Stability Theory. In *Model-Reference Adaptive Control: A Primer*; Springer International Publishing: Cham, Switzerland, 2018; pp. 47–81. [\[CrossRef\]](#)
11. Lyapunov, A. A General Task about the Stability of Motion. Ph.D. Thesis, University of Kazan, Tatarstan, Russia, 1892. (In Russian)

12. Lyapunov, A. *Stability of Motion*; Academic Press: New York, NY, USA; London, UK, 1966.
13. Muthukumar, N.; Srinivasan, S.; Ramkumar, K.; Kannan, K.; Balas, V. Adaptive Model Predictive Controller for Web Transport Systems. *Acta Polytech. Hung.* **2016**, *13*, 181–194. [[CrossRef](#)]
14. Reda, A.; Bouzid, A.; Vásárhelyi, J. Model Predictive Control for Automated Vehicle Steering. *Acta Polytech. Hung.* **2020**, *17*, 163–182. [[CrossRef](#)]
15. Gahinet, P.; Apkarian, P.; Chilali, M. Affine parameter-dependent Lyapunov functions and real parametric uncertainty. *IEEE Trans. Autom. Control.* **1996**, *41*, 436–442. [[CrossRef](#)]
16. Tar, J.; Bitó, J.; Nádai, L.; Tenreiro Machado, J. Robust Fixed Point Transformations in Adaptive Control Using Local Basin of Attraction. *Acta Polytech. Hung.* **2009**, *6*, 21–37.
17. Liu, Y.; Yu, H. A survey of underactuated mechanical systems. *IET Control Theory Appl.* **2013**, *7*, 921–935. [[CrossRef](#)]
18. Spong, M. Partial feedback linearization of underactuated mechanical systems. In Proceedings of the IEEE/RSJ International Conference on Intelligent Robots and Systems (IROS'94), Munich, Germany, 12–16 September 1994; Volume 1, pp. 314–321. [[CrossRef](#)]
19. Spong, M.W. Energy Based Control of a Class of Underactuated Mechanical Systems. *IFAC Proc. Vol.* **1996**, *29*, 2828–2832.
20. Olfati-Saber, R. Nonlinear Control of Underactuated Mechanical Systems with Application to Robotics and Aerospace Vehicles. Ph.D. Thesis, Department of Electrical Engineering and Computer Science, Massachusetts Institute of Technology, Cambridge, MA, USA, 2001.
21. Lai, X.Z.; She, J.H.; Yang, S.X.; Wu, M. Comprehensive Unified Control Strategy for Underactuated Two-Link Manipulators. *IEEE Trans. Syst. Man, Cybern. Part B Cybernetics* **2009**, *39*, 389–398. [[CrossRef](#)]
22. Freidovich, L.; Shiriaev, A.; Gordillo, F.; Gomez-Estern, F.; Aracil, J. Partial-energy-shaping control for orbital stabilization of high frequency oscillations of the Furuta pendulum. In Proceedings of the 2007 46th IEEE Conference on Decision and Control, New Orleans, LA, USA, 12–14 December 2007; pp. 4637–4642. [[CrossRef](#)]
23. Gao, B.; Zhang, X.; Chen, H.; Zhao, J. Energy-based control design of an underactuated 2-dimensional TORA system. In Proceedings of the 2009 IEEE/RSJ International Conference on Intelligent Robots and Systems, St. Louis, MO, USA, 10–15 October 2009; pp. 1296–1301. [[CrossRef](#)]
24. Ortega, R.; García-Canseco, E. Interconnection and Damping Assignment Passivity-Based Control: A Survey. *Eur. J. Control.* **2004**, *10*, 432–450. [[CrossRef](#)]
25. Bloch, A.; Leonard, N.; Marsden, J. Controlled Lagrangians and the stabilization of mechanical systems. I. The first matching theorem. *IEEE Trans. Autom. Control* **2000**, *45*, 2253–2270. [[CrossRef](#)]
26. Kokotovic, P.; Krstic, M.; Kanellakopoulos, I. Backstepping to passivity: Recursive design of adaptive systems. In Proceedings of the [1992] Proceedings of the 31st IEEE Conference on Decision and Control, Tucson, AZ, USA, 16–18 December 1992; Volume 4, pp. 3276–3280. [[CrossRef](#)]
27. McNinch, L.C.; Ashrafiuon, H. Predictive and sliding mode cascade control for Unmanned Surface Vessels. In Proceedings of the 2011 American Control Conference, San Francisco, CA, USA, 29 June–1 July 2011; pp. 184–189. [[CrossRef](#)]
28. Aloui, S.; Pagès, O.; Hajjaji, A.E.; Chaari, A.; Koubaa, Y. Robust Adaptive Fuzzy Sliding Mode Control Design for a class of MIMO underactuated system. *IFAC Proc. Vol.* **2011**, *44*, 11127–11132.
29. Krafes, S.; Chalh, Z.; Saka, A. A Review on the Control of Second Order Underactuated Mechanical Systems. *Complexity* **2018**, *2018*, 9573514. [[CrossRef](#)]
30. Rekabi, F.; Shirazi, F.A.; Sadigh, M.J.; Saadat, M. Nonlinear H_∞ Measurement Feedback Control Algorithm for Quadrotor Position Tracking. *J. Frankl. Inst.* **2020**, *357*, 6777–6804. [[CrossRef](#)]
31. Krstic, M.; Kanellakopoulos, I.; Kokotovic, P. *Nonlinear and Adaptive Control Design*; Wiley-Interscience: New York, NY, USA, 1995.
32. Mirkin, B.; Gutman, P.O.; Shtessel, Y. Robust adaptive tracking with an additional plant identifier for a class of nonlinear systems. *J. Frankl. Inst.* **2010**, *347*, 974–987.
33. Deutschmann, B.; Ott, C.; Monje, C.; Balaguer, C. Robust Motion Control of a Soft Robotic System Using Fractional Order Control. In *Advances in Service and Industrial Robotics—Proc. of the 26th International Conference on Robotics in Alpe-Adria-Danube Region (RAAD 2017)*, 21–23 June 2017, Torino, Italy; Ferraresi, C., Quaglia, G., Eds.; Springer: Cham, Switzerland, 2017; pp. 142–149. [[CrossRef](#)]
34. Bruzzone, L.; Belotti, V.; Fanghella, P. Implementation of a fractional-order control for robotic applications. In *Advances in Service and Industrial Robotics—Proc. of the 26th International Conference on Robotics in Alpe-Adria-Danube Region (RAAD 2017)*, 21–23 June 2017, Torino, Italy; Ferraresi, C., Quaglia, G., Eds.; Springer: Cham, Switzerland, 2017; pp. 160–167. [[CrossRef](#)]
35. Tenreiro Machado, J.; Kiryakova, V. The Chronicles of Fractional Calculus. *Fract. Calc. Appl. Anal.* **2017**, *20*, 307–336. [[CrossRef](#)]
36. Varga, B.; Horváth, R.; Tar, J.K. Fractional Order Calculus-Inspired Kinematic Design in Adaptive Control. In *Advances in Service and Industrial Robotics*; Müller, A., Brandstötter, M., Eds.; Springer: Cham, Switzerland, 2022; pp. 218–225. [[CrossRef](#)]
37. Atinga, A.; Bitó, J.F.; Tar, J.K. On the Simulation of Lower Order Control Strategies for Higher Order Systems. In Proceedings of the IEEE Joint 22nd International Symposium on Computational Intelligence and Informatics and 8th International Conference on Recent Achievements in Mechatronics, Automation, Computer Science and Robotics (CINTI-MACRO 2022), Budapest, Hungary, 21–22 November 2022; IEEE: New York, NY, USA, 2022; pp. 119–124.
38. Kovács, L.; Eigner, G.; Czakó, B.; Siket, M.; Tar, J. An opportunity of using Robust Fixed Point Transformation-based controller design in case of Type 1 Diabetes Mellitus. In Proceedings of the 2019 First International Conference on Societal Automation (SA), Krakow, Poland, 4–6 September 2019; pp. 1–7. [[CrossRef](#)]

39. Varga, B.; Horváth, R.; Tar, J.K. Adaptive Control of a Nonlinear System Avoiding State Estimation. In Proceedings of the 2022 IEEE 20th Jubilee World Symposium on Applied Machine Intelligence and Informatics (SAMI), Poprad, Slovakia, 2–5 March 2022; pp. 000323–000328. [[CrossRef](#)]
40. Kovacs, A.; Vajk, I. Tuning Parameter-free Model Predictive Control with Nonlinear Internal Model Control Structure for Vehicle Lateral Control. *Acta Polytech. Hung.* **2023**, *20*, 185–204. [[CrossRef](#)]
41. Banach, S. Sur les opérations dans les ensembles abstraits et leur application aux équations intégrales (About the Operations in the Abstract Sets and Their Application to Integral Equations). *Fund. Math.* **1922**, *3*, 133–181. [[CrossRef](#)]
42. Dineva, A.; Tar, J.K.; Várkonyi-Kóczy, A. Novel Generation of Fixed Point Transformation for the Adaptive Control of a Nonlinear Neuron Model. In Proceedings of the 2015 IEEE International Conference on Systems, Man, and Cybernetics, Hong Kong, China, 9–12 October 2015; pp. 987–992. [[CrossRef](#)]
43. Dineva, A.; Tar, J.K.; Várkonyi-Kóczy, A.; Piuri, V. Generalization of a sigmoid generated Fixed Point Transformation from SISO to MIMO systems. In Proceedings of the 2015 IEEE 19th International Conference on Intelligent Engineering Systems (INES), Bratislava, Slovakia, 3–5 September 2015; pp. 135–140. [[CrossRef](#)]
44. Csanádi, B.; Galambos, P.; Tar, J.K.; Györök, G.; Serester, A. A Novel, Abstract Rotation-Based Fixed Point Transformation in Adaptive Control. In Proceedings of the 2018 IEEE International Conference on Systems, Man, and Cybernetics (SMC), Miyazaki, Japan, 7–10 October 2018; pp. 2577–2582. [[CrossRef](#)]
45. Lovas, I. Fixed Point, Iteration-based, Adaptive Controller Tuning, Using a Genetic Algorithm. *Acta Polytech. Hung.* **2022**, *19*, 59–77. [[CrossRef](#)]
46. Tar, J.K.; Bitó, J.F.; Rudas, I.J. Replacement of Lyapunov’s direct method in Model Reference Adaptive Control with Robust Fixed Point Transformations. In Proceedings of the 2010 IEEE 14th International Conference on Intelligent Engineering Systems, Las Palmas, Spain, 5–7 May 2010; pp. 231–235. [[CrossRef](#)]
47. Kalita, B.; Dwivedy, S. Nonlinear dynamics of a parametrically excited pneumatic artificial muscle (PAM) actuator with simultaneous resonance condition. *Mech. Mach. Theory* **2019**, *135*, 281–297. [[CrossRef](#)]
48. Bíró, I.; Trojanová, M.; Čakurda, T.; Fabulya, Z.; Sárossi, J. Simulation of the Position Control of PAM, Using Its Nonlinear Dynamic Model. *Acta Polytech. Hung.* **2023**, *20*, 103–123. [[CrossRef](#)]
49. Szuchy, P.; Cveticanin, L.; Bíró, I. Multi Cantilever-Mass Mechanism for Vibration Suppression. *Acta Polytech. Hung.* **2022**, *19*, 197–212. [[CrossRef](#)]
50. Fajtli, T. *Robotkar Dinamikai Szabályozásának Szimulációs Összehasonlító Vizsgálata “Fixpont Transzformációs Adaptív” és “Fixpont Transzformáció Alapuló Modell Referenciás Adaptív (MRAC)” szabályozóval, Tudományos Diákköri Dolgozat [Simulation-Based Comparison of Fixed Point Iteration-Based Adaptive and Model Reference Adaptive Dynamic Control of a Robot Arm (Scientific Students’ Conference, 2017, Budapest, Hungary)]*; Óbuda University: Budapest, Hungary, 2017. (In Hungarian)

Disclaimer/Publisher’s Note: The statements, opinions and data contained in all publications are solely those of the individual author(s) and contributor(s) and not of MDPI and/or the editor(s). MDPI and/or the editor(s) disclaim responsibility for any injury to people or property resulting from any ideas, methods, instructions or products referred to in the content.